POLITECNICO DI TORINO

Dipartimento di Ingegneria Meccanica e Aerospaziale

Corso di Laurea Magistrale
in Ingegneria Aerospaziale

Tesi di Laurea Magistrale

Analysis of Electric Propulsion transfers for multiple debris removal

Relatore | **Candidato**

prof. Lorenzo Casalino | Biagio Cotugno

Marzo 2018

Summary

Index of figures

Index of tables

1 Introduction

La copiosa presenza nello spazio di detriti o "spazzatura" – come meno elegantemente viene di solito indicato tutto quel complesso di frammenti dispersi nello spazio, creati dall'uomo ma che a quest'ultimo non servono più – è un problema attuale che vede coinvolti da anni gli scienziati delle agenzie spaziali di tutto il mondo: un complesso di scarti potenzialmente pericolosi per le successive rotte di osservazione spaziale, in particolar modo in orbita LEO.

Tale problematica, sempre più all'ordine del giorno, è conseguente e strettamente collegata all'aumento esponenziale delle missioni spaziali dopo il lancio di Sputnik 1 che ha portato in orbita una quantità sempre maggiore di "*space junk*" come ultimi stadi di lanciatori, parti di satelliti o satelliti non più operanti, oltre che da detriti generati da collisioni nello spazio: tutto questo insieme di "immondizia spaziale" (termine preso a prestito dalle relazioni dei più autorevoli scienziati) cosituisce un ostacolo ed un concreto rischio sia per il lancio di nuovi satelliti che per la sicurezza della *crew* a bordo di uno *spacecraft* per una missione con equipaggio.

La propulsione elettrica rappresenta una nuova frontiera per lo spazio ed una valida alternativa all'uso a bordo della propulsione chimica. In tale prospettiva notevoli passi avanti sono stati fatti dopo i primi studi eseguiti dallo scienziato statunitense Robert H. Goddard (1882-1945) e dopo i primi esperimenti a bordo del SERT-1 che hanno portato i propulsori elettrici a poter essere utilizzati anche per missioni a breve termine nonostante la produzione della loro spinta sia modesta in quanto diretta conseguenza della potenza generabile a bordo (principalmente per mezzo di pannelli solari).

In questa lavoro viene presentato uno studio di missione che ha per oggetto la rimozione di *multiple debris* in orbita bassa attorno alla terra, sfruttando un *chaser* equipaggiato con propulsione elettrica ed un *kit* operante con propulsione chimica.

Lo studio è stato sviluppato sfruttando un algoritmo ed un modello matematico per la risoluzione dei problemi di Keplero e Lambert che - a partire dalla definizione delle variabili in gioco, dei valori iniziali e finali delle condizioni al contorno - andasse iterativamente ad annullare l'errore tra:

- la posizione calcolata del chaser rispetto al debris di arrivo
- la posizione ottenuta tenendo conto delle perturbazioni secolari agenti sul nodo ascendente e sull'argomento del periastro dell'orbita dello spacecraft.

L'analisi tende ad esaminare, in primo luogo, tutte le possibili sequenze caratterizzate da un tempo di missione non superiore a 6 mesi (180 giorni) e da un consumo - in termini di ΔV - inferiore ad 1.5 km/s, arrivando ad eliminare tutte quelle sequenze considerate "errate" (ossia caratterizzate da passaggi multipli per lo stesso debris o quelle con tempo di rendez-vous tra un detrito e l'altro inferiore al tempo necessario per effettuare la manovra con propulsione elettrica).

Nel presente studio tali sequenze, calcolate per diversi valori di accelerazione dello spacecraft, sono state in via successiva ottimizzate sia in termini di tempo di missione che di consumo di propellente ed i relativi risultati sono stati rapportati e confrontati con quelli ottenuti attraverso una medesima missione effettuata, però, con la propulsione chimica.

È stato, ancora, sviluppato un *mass budget* per le varie tipologie di propulsori oggetto di studio che ha dovuto tener conto della potenza necessaria al funzionamento del propulsore elettrico, per poi comparare le differenze ottenute con la stessa missione effettuata con propulsore chimico, evidenziandone i rispettivi dati positivi e di criticità.

Le sequenze simili, infine, sono state ulteriormente selezionate ed equiparate tra loro per poter eseguire una valutazione obiettiva sui differenti risultati al fine di individuare il miglior processo di rimozione dei detriti in termini di tempo di missione e di consumo di propellente.

The copious presence of debris in space or "garbage" - as less elegantly it is usually indicated all the complex of fragments dispersed in space, created by man but that is no longer needed by the man - is a current problem that involves scientists from space agencies all over the world: a complex of potentially dangerous waste for the subsequent space observation routes, in particular in LEO orbit.

This problem is still commonplace and is consequent and closely linked to the exponential increase in space missions after the launch of Sputnik 1 which has brought an ever-increasing amount of space junk into orbit as the last stages of launchers, parts of satellites or no longer operating satellites, as well as debris generated by collisions in space: all this set of "space garbage" (term borrowed from the reports of the most authoritative scientists) constitutes an obstacle and a concrete risk for both the launch of new satellites for the safety of the crew on board a spacecraft for a manned mission.

Electric propulsion represents a new frontier for space and a valid alternative to the use on board of chemical propulsion. In this perspective, considerable progress has been made after the first studies carried out by the American scientist Robert H. Goddard (1882-1945) and after the first experiments on board the SERT-1 that led the electric propulsion to be used for short missions too, despite the production of their thrust is modest as a direct consequence of the power that can be generated on board (mainly with solar panels).

In this paper, a mission study is presented that deals with the removal of multiple debris in a low orbit around the earth, exploiting a chaser equipped with electric propulsion and a kit operating with chemical propulsion.

The study was developed using an algorithm and a mathematical model for solving Kepler and Lambert problems that - starting from the definition of the variables involved, the initial and final values of the boundary conditions - was run iteratively to nullify the error between:

- the calculated position of the chaser with respect to the arrival debris
- the position obtained taking into account the secular perturbations acting on the ascending node and on the argument of periapsis of the spacecraft orbit.

The analysis tends to examine, in first place, all the possible sequences characterized by a mission time not exceeding 6 months (180 days) and by a consumption - in terms of ΔV - less than 1.5 km /s, eventually deleting all those "incorrect" sequences (i.e. characterized by multiple passages for the same debris or those with a time of rendezvous between a debris and another shorter than the time necessary to perform the manoeuvre with electric propulsion).

In the present study, these sequences, calculated for different acceleration values of the spacecraft, were subsequently optimized both in terms of mission time and propellant consumption and the relative results were compared and matched with those obtained through the same mission carried out with the chemical propulsion.

A mass budget has been developed too, taking into account the necessary power for the electric propulsion engines, to compare the differences obtained with the same mission carried out with a chemical engine, highlighting the respective positive and critical data.

Finally, similar sequences have been further selected and compared to each other in order to perform an objective evaluation of the different results to identify the best debris removal process in terms of mission time and propellant consumption.

2 Debris and debris removal

More than 20.000 tons of natural (*dust*, *meteoroids*, *micrometeoroids*, chunks of *asteroids*, *comets*) and man-made objects hit the Earth every year.

Meteoroids are in orbit around the sun, while most artificial debris are in orbit around the Earth. Hence, the latter is more commonly referred to as orbital debris.

With every mission, parts of satellites, satellites, pieces of old exhausted booster segments and even astronauts' equipment (such as astronaut Ed White's glove from first extra-vehicular activity of 1965 Gemini 4 flight or Gene Rodenberry's ashes, creator of the Star Trek series) have remained in space so that the environment around Earth is filling up with "junk" which constitutes an increasing risk for manned and unmanned space missions.

Even tiny paint flecks can damage a spacecraft when traveling at these velocities (34.500 km/h). The fused-silica and borosilicate-glass window of the ISS cupola has been damaged for a 7-mm wide dent. In fact, a number of space shuttle windows have been replaced because of damage caused by material that was analysed and shown to be paint flecks.

Current estimations say that there are over 170 million debris smaller than 1cm, 670.000 debris between 1 cm and 10 cm and 29.000 debris larger than 10 cm orbiting around Earth. Among these, 16.000 are man-made non-operational objects that have been tracked by the US Strategic Command.

Collision risks are divided into three categories depending upon size of threat. For objects 10 centimetres and larger, conjunction assessments and collision avoidance manoeuvres are effective in countering objects which can be tracked by the Space Surveillance Network. Objects smaller than this usually are too small to track and too large to shield against. Debris shields can be effective in withstanding impacts of particles smaller than 1 centimetre.

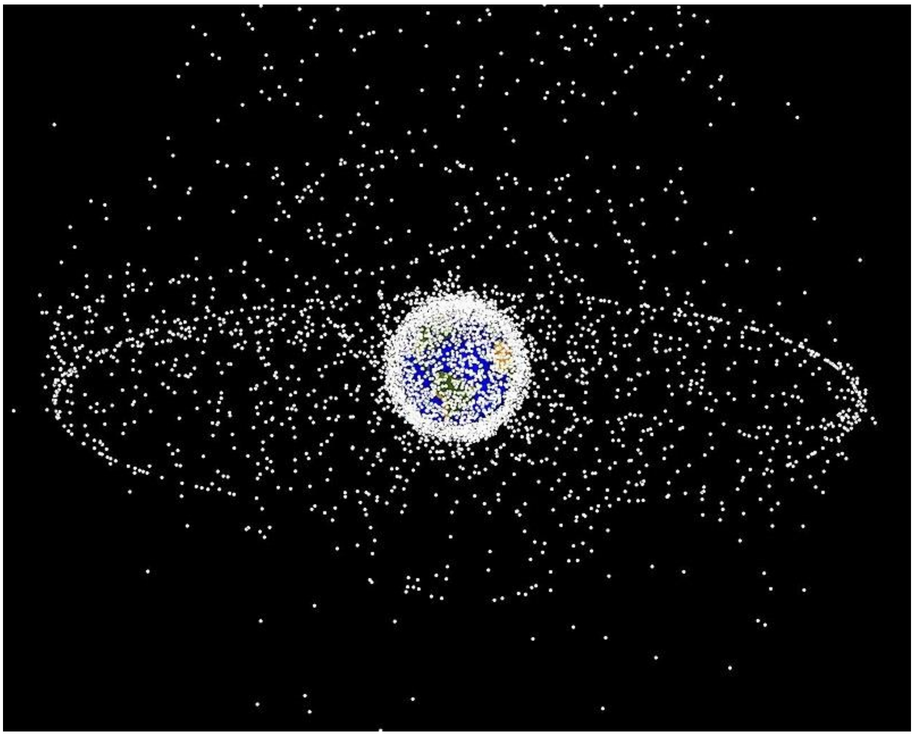

Figure 1: Space debris population

According to Donald J. Kessler (1940 -) the scenario of space debris in low earth orbit is so dense of debris that the number of collisions grow exponentially every year so that new debris born from their impact, increasing the risk of new collisions (chain reaction) and making future space missions harder to accomplish.

Relative velocities in low orbits are up to 57.600 km/h (16 km/s) so that the kinetic energy of the collision between two “big enough” objects (diameter larger than 10 cm) creates a cloud of debris in the form of splinters launched in random directions.

Each fragment therefore has the potential to induce further impacts, creating an even greater number of spatial debris. With a large collision (for example between a space station and a non-operative satellite), the amount of debris could be sufficient to make the low orbit level virtually unattainable.

However, the Kessler syndrome’s risk does not completely apply to debris in lower orbits because of the atmospheric drag: the resistance they encounter gradually lowers their altitude until they burn in the atmosphere, thus keeping the area clear of waste. Collisions that occur below this altitude are not a problem, since the loss of energy in the collision causes the debris orbit to have a perigee below that altitude.

At higher altitudes, where the atmospheric drag is not so significant, the time the debris stay in orbit around Earth is considerable. The influence of the moon, solar wind and weak atmospheric drag slowly lower debris orbits up to where they naturally burn but this process can take millenniums to occur.

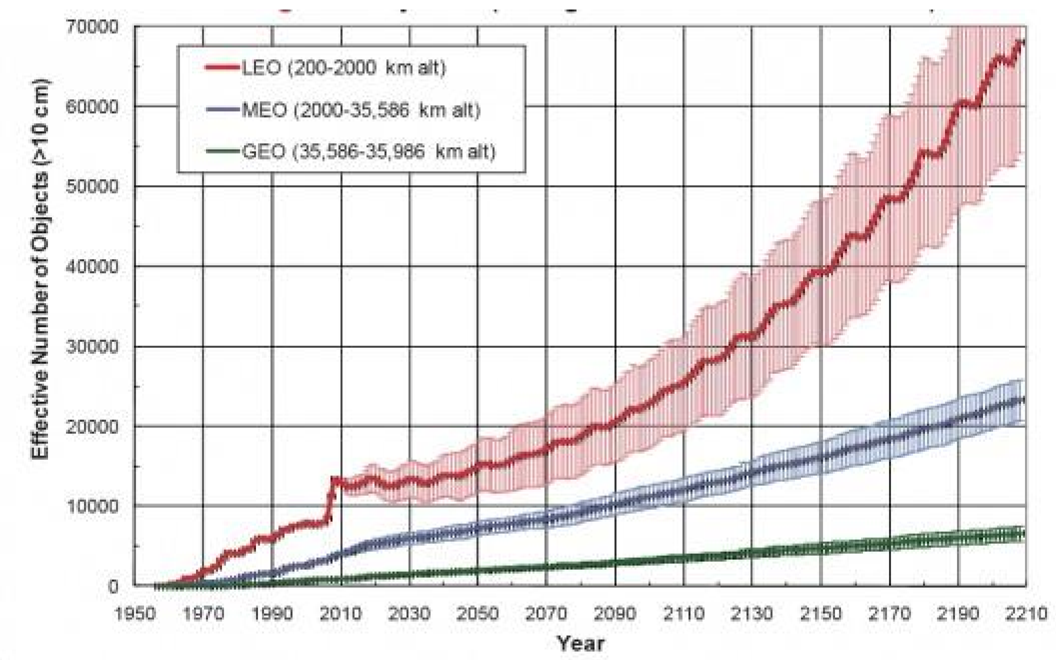

Figure 2: Kessler's syndrome trend

To reduce the generation of additional space debris, countermeasures can be taken into account:

- *Passivation* of the spacecraft, i.e. expulsion of excess fuel once the operations have been completed to eliminate (or at least reduce to a minimum) the risk of explosions in orbit which would generate a huge amount of debris.
- In the event that the deorbit is too expensive, it could lead the satellite to orbit at a *lower altitude* so that the deorbit of the same occurs naturally (passive deorbit) in a maximum of 15 years (according to ESA specifications).

- Introduction of *parking orbits* (graveyard orbits) for satellites orbiting too high to carry out active or passive deorbit (e.g. for satellites operating in geostationary or geosynchronous orbits).
- Debris removal with specific missions.

For what concerns the plan for reacting to debris, NASA has developed a set of long-standing guidelines used to assesses whether the treat of a close passage to the debris is sufficient to warrant evasive manoeuvres to ensure the safety of the spacecraft and the crew (in case of a manned mission).

"*Debris avoidance manoeuvres are planned when the probability of collision from a conjunction reaches limits set in the space shuttle and space station flight rules. If the probability of collision is greater than 1 in 100.000, a maneuver will be conducted if it will not result in significant impact to mission objectives. If it is greater than 1 in 10.000, a manoeuvre will be conducted unless it will result in additional risk to the crew.*

Debris avoidance manoeuvres are usually small and occur from one to several hours before the time of the conjunction. Debris avoidance manoeuvres with the shuttle can be planned and executed in a matter of hours. Such manoeuvres with the space station require about 30 hours to plan and execute mainly due to the need to use the station's Russian thrusters, or the propulsion systems on one of the docked Russian or European spacecraft.

Several collision avoidance manoeuvres with the shuttle and the station have been conducted during the past 10 years.

NASA implemented the conjunction assessment and collision avoidance process for human spaceflight beginning with shuttle mission STS-26 in 1988. Before launch of the first element of the International Space Station in 1998, NASA and DoD jointly developed and implemented a more sophisticated and higher fidelity conjunction assessment process for human spaceflight missions.

In 2005, NASA implemented a similar process for selected robotic assets such as the Earth Observation System satellites in low Earth orbit and Tracking and Data Relay Satellite System in geosynchronous orbit.

In 2007, NASA extended the conjunction assessment process to all NASA manoeuvrable satellites within low Earth orbit and within 124 miles (200 kilometres) of geosynchronous orbit.

DoD's Joint Space Operations Center (JSpOC) is responsible for performing conjunction assessments for all designated NASA space assets in accordance with an established schedule (every eight hours for human spaceflight vehicles and daily Monday through Friday for robotic vehicles). JSpOC notifies NASA (Johnson Space Center for human spaceflight and Goddard Space Flight Center for robotic missions) of conjunctions which meet established criteria.

JSpOC tasks the Space Surveillance Network to collect additional tracking data on a threat object to improve conjunction assessment accuracy. NASA computes the probability of collision, based upon miss distance and uncertainty provided by JSpOC.

Based upon specific flight rules and detailed risk analysis, NASA decides if a collision avoidance manoeuvre is necessary.

If a manoeuvre is required, NASA provides planned post-manoeuvre orbital data to JSpOC for screening of near-term conjunctions. This process can be repeated if the planned new orbit puts the NASA vehicle at risk of future collision with the same or another space object." [Ref. NASA]

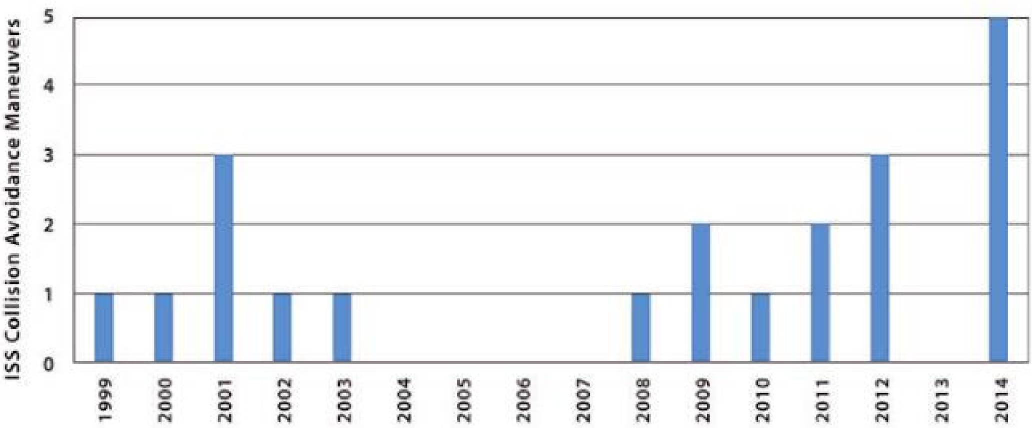

Figure 3: Frequency of ISS collision avoidance manoeuvres between 1999 and 2014 (Image credit: NASA)

3 Mathematical model

3.1 Orbit perturbations

Ideal Keplerian orbits assume that the motion of a spacecraft (in general of a body) in its orbit is the result of the attraction between two bodies only.

There are nonconservative perturbing forces, such as solar pressure that tend to change the eccentricity (e) of the spacecraft orbit or the atmospheric drag that tend to decrease the major axis (a) of the orbit causing the satellite to fall back to the earth's surface.

These perturbations can be classified on how they affect the Keplerian elements:

- *secular variations* coincide with a linear variation of the orbital elements
- *short-period variations* that tend to repeat periodically with a period less than the orbit period
- *long-period variations* are the perturbations that repeat periodically with a period greater than the orbit one.

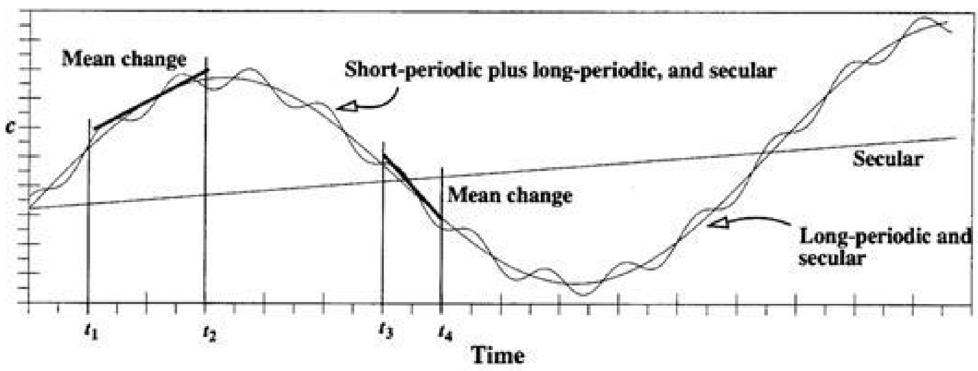

Figure 4: Effect of perturbations forces on orbital elements

The change in any orbital element, c, is here illustrated. The straight line shows the secular effect. The large oscillating line shows the secular plus long-period effects and the small oscillatory line, which combines all three, shows the short-period effects.

The perturbations due to the oblateness of the Earth are the results of assuming that the Earth is not perfectly spherically symmetrical or homogenous in mass: in fact, the Earth has a bulge on the equator and is crushed at the poles.

Table 1: Earth flattening

Earth equatorial radius (R)	6378.388 km
Earth polar radius (R')	6356.912 km
Earth flattening	$(R - R')/R = 0.003$

The potential generated by the oblateness of the Earth causes both secular and periodical perturbation.

By using the zonal coefficient J_n for defyning the potential function of the Earth, the results of the non-spherical Earth take into account the J_2 coefficient in the geopotential expansion.

Secular variations due to J2 affect only the longitude of the ascending node (Ω), the argument of perigee (ω) and the mean anomaly (M). These variations are the results of the gyroscopic precession of the orbit around the ecliptic pole.

The rates of change of longitude of ascending node (Ω) and argument of periapsis (ω) are as follows:

$$\Omega_{J_2} = -\frac{3}{2}\frac{nJ_2\cos(i)}{(1-e^2)^2}\left(\frac{R_e}{a}\right)^2$$

$$\omega_{J_2} = -\frac{3}{4}\frac{nJ_2[1-5\cos^2 i]}{(1-e^2)^2}\left(\frac{R_e}{a}\right)^2$$

where n is the mean motion in degrees/day, J_2 has the value of 0.001082629, R_e is the Earth equatorial radius of 6378.1363 km, a is the sami-major axis in km, i is the inclination in degrees, e is the eccentricity and Ω and ω are in degrees/day.

Before launching the analysis, the perturbation of the Right Ascension of the Ascending Node (RAAN – Ω [deg]), in terms of variation of RAAN over time ($\dot{\Omega}$), has been studied.

A perturbation is a deviation from normal or expected motion (deviation from expected orbital elements). When analysing the universe from an accurate point of view, one can distinct, sometimes unpredictably, some irregularities of motion upon the mean motion of celestial bodies.

Some of the perturbations that can be considered are mainly due to attracting bodies, atmospheric drag and lift, asphericity of celestial bodies (e.g. the Earth), solar effects (radiation, magnetism).

For this mission scenario, the perturbation of the orbital elements over time is a problem related to the Earth flattening only (because of the low orbit of the chaser satellite) and has been solved by evaluating the daily perturbation of the RAAN parameter. Ignoring this effect would cause us to completely fail in the prediction of the satellite position over time.

The variation of the Ω parameter directly influences the geometry of the transfer manoeuvre and the ΔV required to the thruster (consumption): the optimal strategy is to wait for the $\Delta\Omega$ – between the two debris – to be null so that no plane change is required but the manoeuvre can be accomplished with a planar transfer.

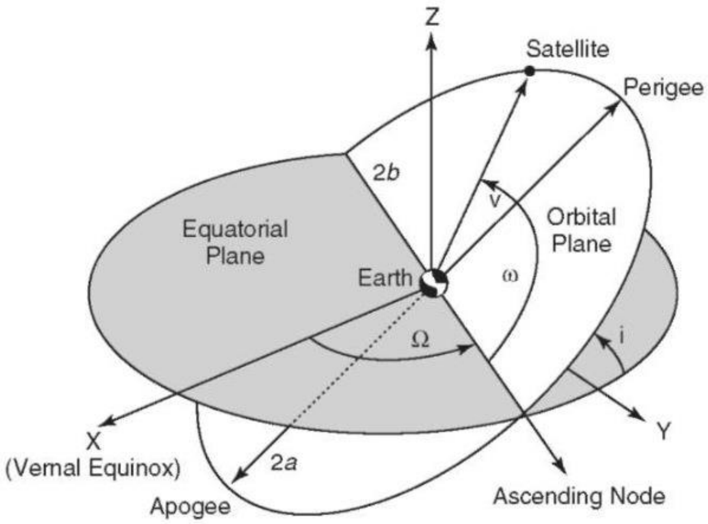

Figure 5: Satellite orbit and orbital elements

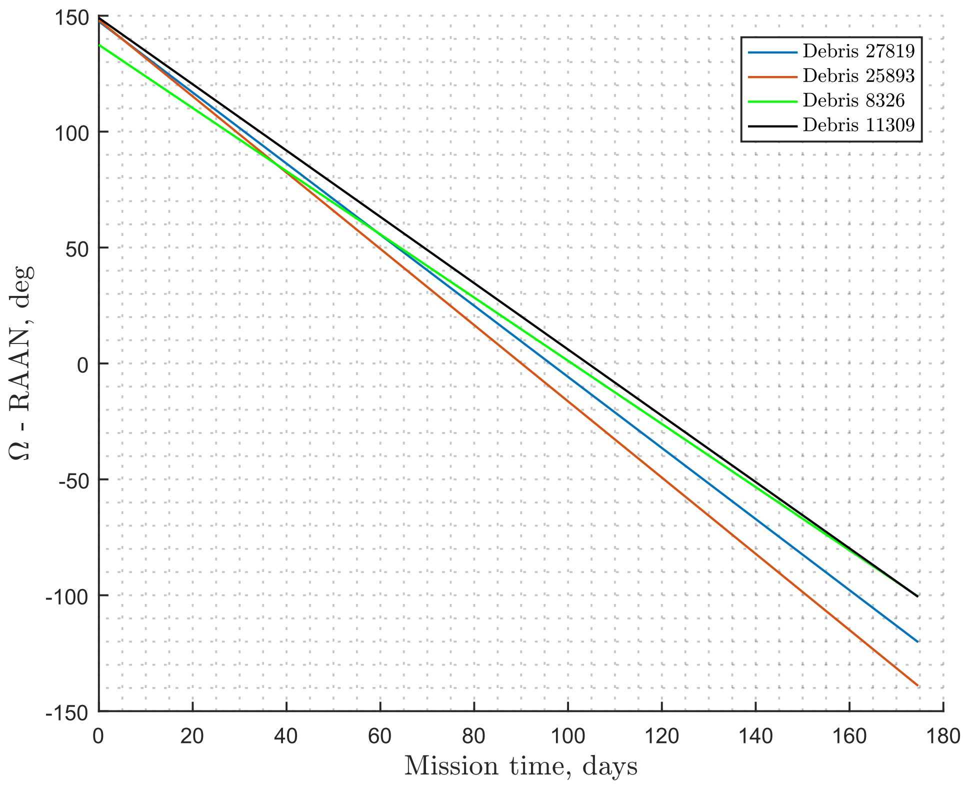

Figure 6: Ascending node variation due to J2 perturbations on 4 debris

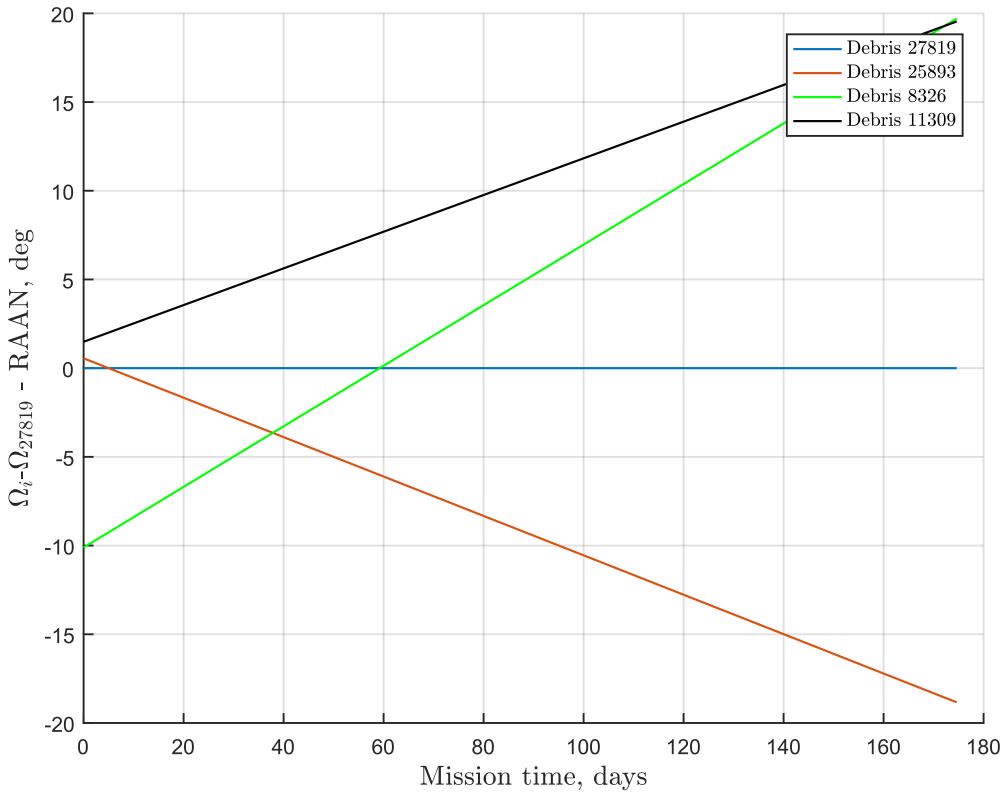

Figure 7: Ascending node variation (related to Debris1) due to J2 perturbations on 4 debris

3.2 *Transfer description for impulsive manoeuvres*

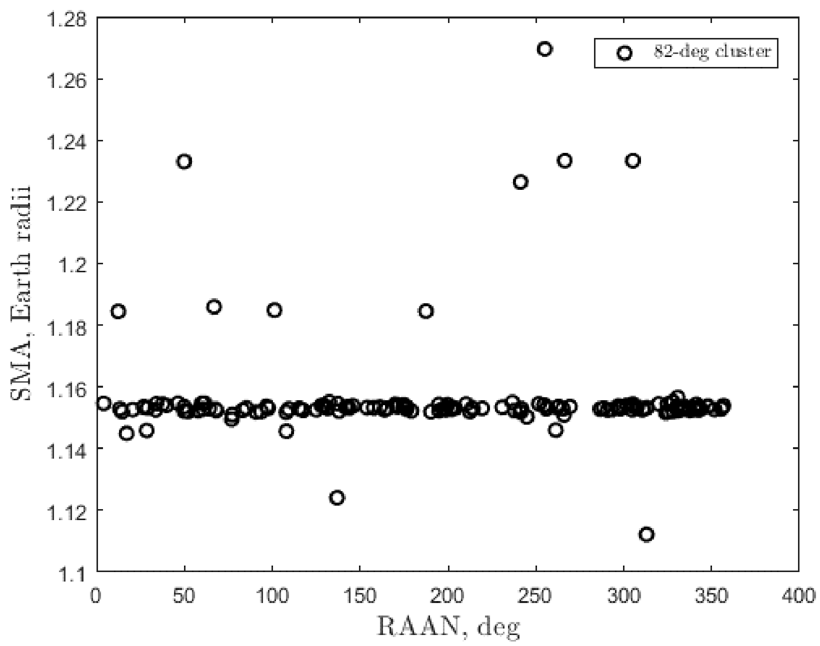

Figure 8: Orbital elements of target set (Epoch 57754 Modified Julian Date)

A population of debris with similar inclination represents the set of possible targets for the space mission.

In this scenario, *Russian Kosmos 3M rocket bodies* – which are a consistent part of large debris population in low earth orbit (LEO) – have been considered.

The United States Strategic command orbital objects database lists more or less 300 Kosmos exhausted rocket bodies orbiting in LEO (listed with the US classification SL-8 R/B).

Starting from identifying two clusters with inclination close to 74 degrees (120 objects) and 82 degrees (156 objects), this study evaluated the cluster of objects orbiting at 82 degrees of inclination.

Departure date is on 1st January 2017: the TLE (two-line elements) of the cluster are first propagated until departure date and then, their orbits are propagated taking into account ideal Keplerian orbits and secular perturbations.

Relevant orbital elements are represented in Figure 8.

Results show that the specific optimal sequences depend strongly on departure date but the general trends can be assumed for any departure date.

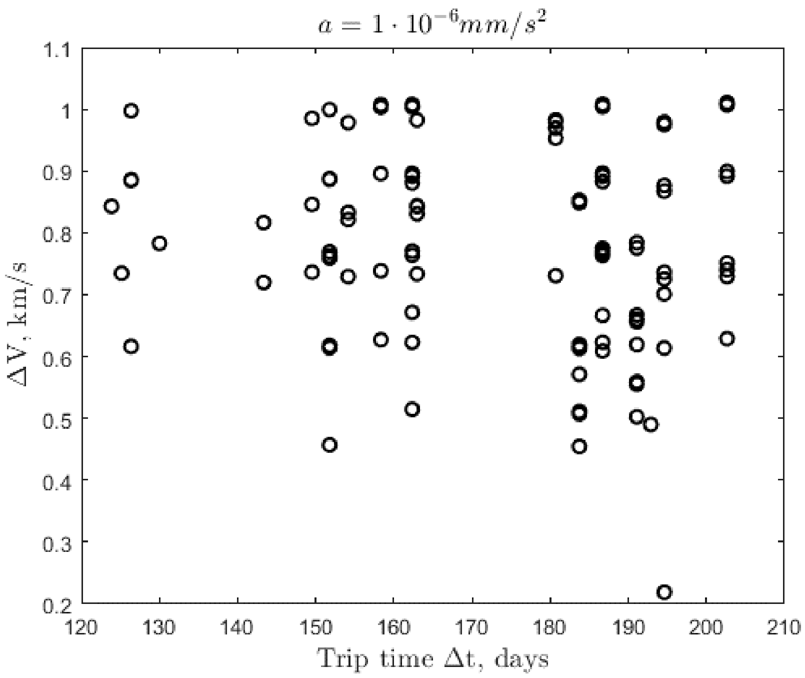

Figure 9: Performance of three-leg sequences for the 82-deg cluster

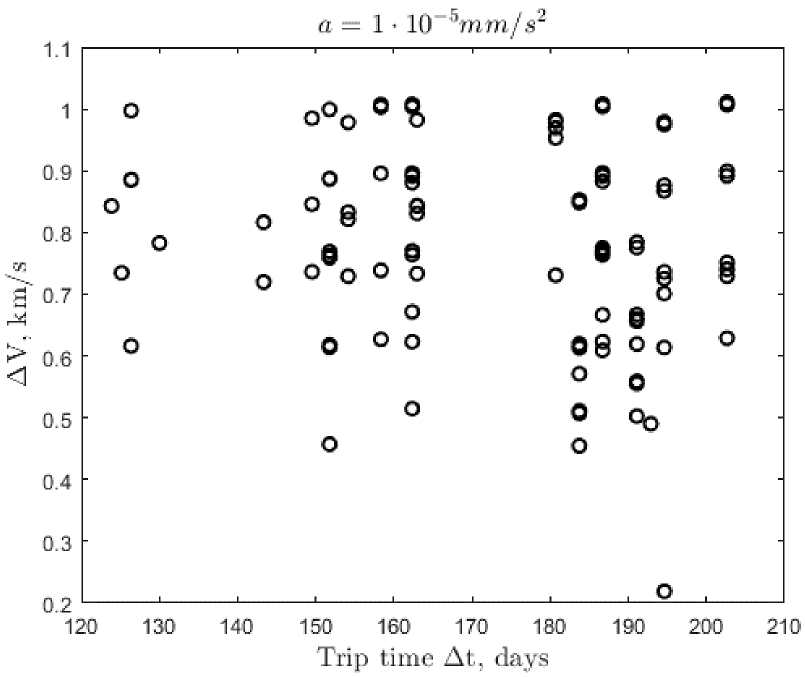

Figure 10: Performance of three-leg sequences for the 82-deg cluster

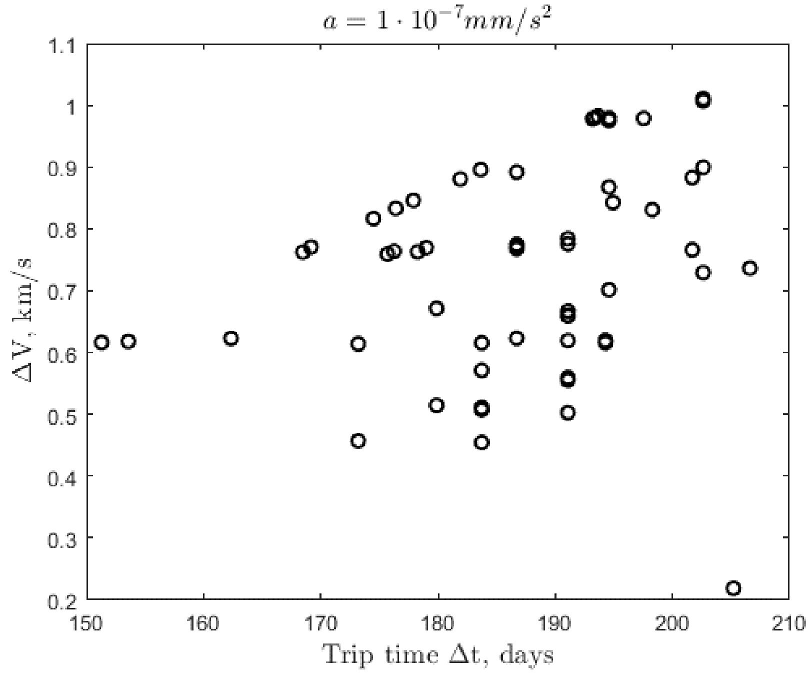

Figure 11: Performance of three-leg sequences for the 82-deg cluster

A complete scan of all the suitable mission opportunities taking into account the variability of departure date and arrival time would be almost impossible.

The global search provides suitable sequences of targets and estimation for rendezvous times and mission cost. It assumes that rendezvous occurs when the orbit planes become coincident and estimates the ΔV as a function of changes in semimajor axis and eccentricity.

The actual mission feasibility and characteristics have been verified by means of an evolutionary algorithm developed at *Politecnico di Torino* used to obtain an optimal solution and so minimum ΔV for each transfer.

The results review provides reliable values with errors of 1-2 days for the times and a few m/s for the ΔV.

It is assumed that the i-th leg begins at the time $\tau_i = t_i$ which derives from the solution of the previous leg and takes into account the moment the orbit planes of the two debris (debris i and debris $i + 1$) coincide and the servicing time.

The times at which performing thrust are lower than the times $\tau_1 < \tau_2 < \tau_3 < \tau_4 = t_{i+1}$ for each leg. The rendezvous time with the last debris $\tau_4 = t_{i+1}$ is an unknown factor of the problem and its value can only be estimated.

Each trip from one debris to another is a problem limited to 10 variables. Three of these define the moments at which performing thrust:

$$p_1 = \tau_4 - \tau_1, p_2 = (\tau_2 - \tau_1)/(\tau_4 - \tau_1), p_3 = (\tau_3 - \tau_2)/(\tau_4 - \tau_2)$$

The flight time p_1 varies in a 10-day window centered in the one suggested by the global search (20 days are used for the longest trip), p_2 and p_3 vary between 0 and 1.

Six variables define the velocity components after the first (marked with the subscript 1+) and the second (marked with the subscript 2+) burn, from the unknown velocity components before these burns (marked with the subscripts 1- and 2- respectively).

$$u_{1+} = u_{1-} + p_4 \sin(p_5)$$

$$v_{1+} = v_{1-} + p_4 \cos(p_5) \cos(\psi + p_6)$$

$$w_{1+} = w_{1-} + p_4 \cos(p_5) \cos(\psi + p_6)$$

$$u_{2+} = u_{2-} + p_7 \sin(p_8)$$

$$v_{1+} = v_{2-} + p_7 \cos(p_8) \cos(\psi + p_9)$$

$$w_{2+} = w_{2-} + p_7 \cos(p_8) \cos(\psi + p_9)$$

$$\psi = \tan^{-1}(w_- / v_-)$$

where u, v and w are the radial, eastward and northward velocity components, and ψ is the heading angle before burn.

p_4 and p_7 are the speed change components ΔV_1 and ΔV_2 that vary between 0 and 800 m/s. p_5 and p_8 are in-plane angles ranging between -180 and 180 deg. p_6 and p_9 are out-of-plane angles ranging from -60 to 60 deg.

Both ΔV and out-of-plane angles are values close to zero (planar trajectories are preferred but a margin on out-of-plane maneuvers must still be considered) to improve the accuracy and convergence of the algorithm.

The last variable p_{10} refers to the last transfer, to perform the rendezvous with the $i + 1$ debris that has a definite position.

For this reason, the Lambert problem must be solved. In this problem multiple revolutions are foreseen and the problem therefore presents two solutions: p_9 is used to choose between the solution of the left branch ($p_{10} < 0.5$) and that of the right branch ($p_{10} > 0.5$).

Once defined the variables of the problem, ΔV of the mission can be evaluated. Initial position, initial time and initial velocity (defined with subscript 1-) are known. Once the speed at the end of the burn is known the Kepler problem can be solved (taking into account the perturbation J_2) to evaluate and calculate position and velocity before the following manoeuvre (2-).

The same procedure is applied to the next arc, allowing to know the position and velocity before the following transfer.

The transfer between point 3 and point 4 (the target debris whose position and velocity are known) is first solved as an unperturbed Lambert problem to obtain the velocity components after the third impulse that would allow to intercept the arrival debris without taking the perturbations into account.

The perturbations J_2 influence the result and therefore an iterative calculation is necessary to nullify the error of the perturbed final position at time t_4 between chaser and target. Total ΔV is:

$$\Delta V = \sum_{j=1}^{4} \Delta V_j = \sum_{j=1}^{4} \sqrt{\left(u_{j+} - u_{j+}\right)^2 + \left(v_{j+} - v_{j+}\right)^2 + \left(w_{j+} - w_{j+}\right)^2}$$

where the values 1- and 4+ are those of the departure and arrival debris.

Each arc is solved in sequence, starting with the values obtained at the end of the previous one.

It is important to note that the optimal strategy for favourable opportunities is often to wait on the initial orbit for a rather long time (i.e. $\Delta V_1 = 0$), until the orbital planes of the two debris coincide, thanks to the perturbations J2.

At this moment the spacecraft performs an impulsive manoeuvre towards the following debris.

3.3 Corrections to the algorithm for Electric Propulsion

Changes were necessary in the algorithm and in the mathematical model, to take into account the use of electric propulsion.

The type of propulsion (chemical or electric) directly influences preliminary results for consumption (propellant mass and ΔV), mass budget and mission time: the starting point of the analysis was to properly write down the characteristic velocity requirement for small changes of quasi-circular orbits.

$$\begin{cases} \dfrac{\Delta V}{V_0} = 0.5\,\dfrac{\Delta a}{a_0} \\ \dfrac{\Delta V}{V_0} = 0.649\ \Delta e \end{cases}$$

and by combining the two formulas:

$$\Delta V = \sqrt{\frac{1}{a_{min}}}\left[0.5\sqrt{a^2} + 0.649\sqrt{\Delta e^2}\right]$$

that represents the formula used in the calculation of the ΔV for the mission with electric propulsion.

The "thrust time" (t_t) has been introduced as an additional parameter of the problem, since the thrust generated by electric propulsion is not impulsive but is defined in a time interval.

The thrust time will modify (and eventually reduce) the possible sequences of debris to be removed because it defines a further comparison parameter in the mission time: if the thrust time is greater than the time necessary to have coincident orbit planes between two debris, the solution will be discarded as it is impossible to perform.

In addition, it is necessary to define a manoeuvre window to univocally identify the temporal instant (defined t_0) in which to start the thrust manoeuvre useful to the rendezvous, so that at the end of the thrust (time t_1) the chaser has correctly performed the rendezvous with the desired debris.

The manoeuvre with electric propulsion is not impulsive but lasts for a certain time span defined by the parameter "thrust time" (t_t). It is impossible to wait for the orbit planes to coincide ($\Delta\Omega = 0$) before starting performing the finite manoeuvre.

During the manoeuvre, the spacecraft leaves the orbit of debris 1 (characterized by Ω_1) and enters the orbit of debris 2 (characterized by Ω_2). It is supposed that the variation of the Ω parameter ($\dot{\Omega}$) is the average between those of the two orbits.

It is desirable that the manoeuvre is centred at the point of coincidence of the orbital planes. There are two relevant cases:

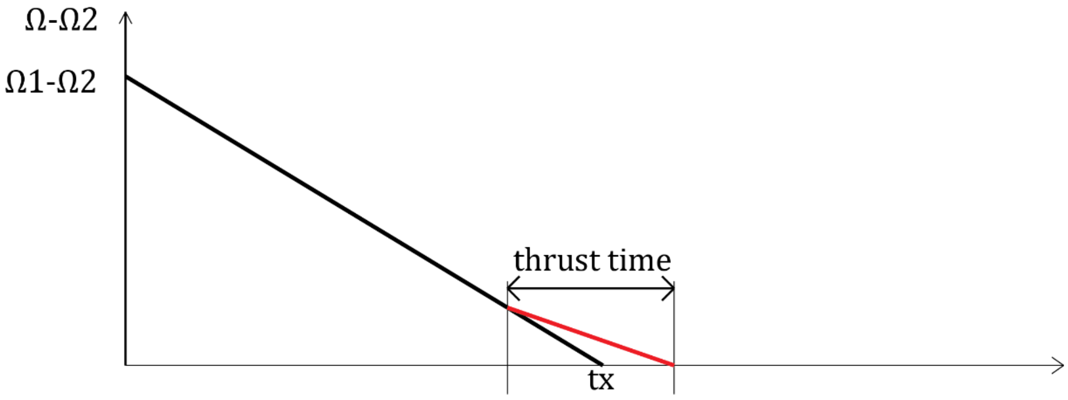

Figure 12:Electric propulsion window manoeuvre for thrust time lower than time necessary to have coincident orbit planes

Thrust time is lower than the time required for the orbit planes to coincide (defined as t_x and so $t_t < t_x$).

The new rendezvous time, taking into account that at time t_x the spacecraft is still performing the manoeuvre, is defined as:

$$t_1 = t_x\left(1 + \frac{1}{2}\frac{t_t}{t_x}\right)$$

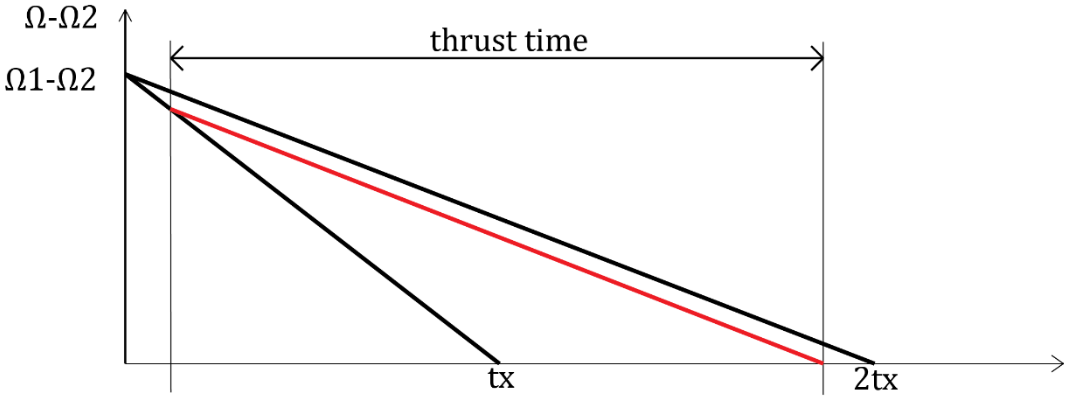

Figure 13: Electric propulsion windows manoeuvre for thrust time greater than the time necessary to have coincident orbit planes but lower than twice it

If the time for the thrust requires more than t_x but less than $2t_x$, it is necessary to evaluate a *waiting time* before starting the rendezvous operation in order to have the centre of the manoeuvre when the orbital planes coincide.

That is to say that the value of $\Omega_1 - \Omega_2$ is strictly dependant on the waiting time (t_w), the thrust time (t_t) and t_x.

In fact:

$$\Delta\Omega = \Omega_1 - \Omega_2 = t_t\left(\frac{\dot{\Omega}_1 - \dot{\Omega}_2}{2}\right) + t_w(\dot{\Omega}_1 - \dot{\Omega}_2) = t_x(\dot{\Omega}_1 - \dot{\Omega}_2) = 0$$

$$t_w = \frac{2t_x - t_t}{2}$$

Or in general:

$$t_1 = t_w + t_t = t_x + \frac{t_t}{2}$$

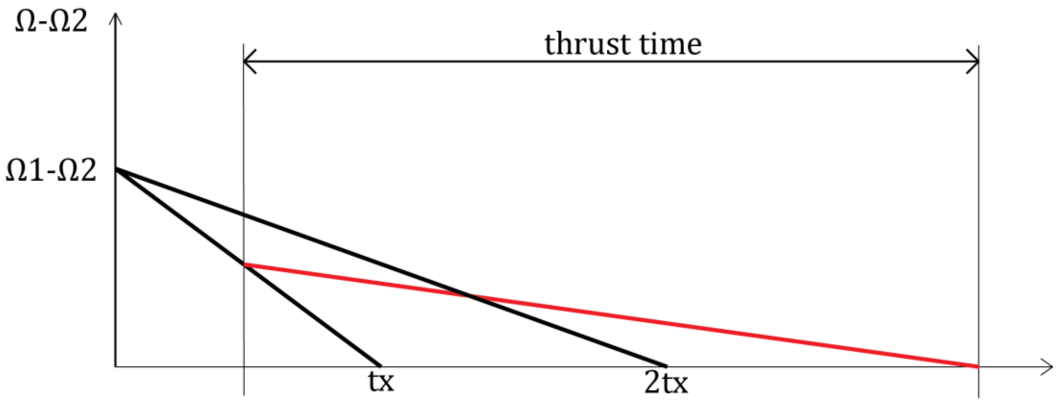

Figure 14:Electric propulsion window manoeuvre for thrust time greater than twice the time necessary to have coincident orbit planes

Instead, if the thrust time is greater than twice the time necessary for the orbit planes to coincide ($t_t > 2t_x$), it is impossible to perform a manoeuvre without a plane change.

The solutions are discarded because there's less time than the necessary one to carry out the rendezvous (the waiting time appears to be negative).

Before compiling the code and running the executable (*.exe), preliminary considerations have been made:

- Different types of electric propulsion based engines have been selected with different specific impulses (I_{sp}) values: Hall thrusters, ion thrusters and arcjets.
- A debris database has been created based on the North America Aerospace Defence Command (NORAD) Catalog Number, containing all the orbital elements (TLE – two-line elements) of n=154 orbiting debris (such as exhausted launchers upper stage) at an inclination of 82 degrees dating back to late 2017.

- Fundamental parameter for the comparison with the chemical propulsion (CP) was the Thrust time because the electric propulsion (EP) requires a finite burn contrary to the chemical propulsion provided by a finite one.
- A 20-day servicing time (DT) was selected, i.e. enough time for scientific operations such as observation and hooking of the debris.
- J2 perturbations have been considered (in other words it was only considered the effect of the Earth flattening on the spacecraft orbiting in LEO). The variation of the Ω parameter over time influences the time of initial burn with electric propulsion. Since the burn is a finite one (and not an impulsive shot) the moment of ignition is certainly earlier than the moment of the impulsive thrust for chemical propulsion.
- i=3 legs have been selected, that is to say, a number of debris m=4 has been chosen providing 154!/150! overall sequences, that is, more than 500 million combinations.
- Before launching the analysis, it was necessary to non-dimensionalize the basic units of measurement to better compare the results for the two propulsions.

4 Electric Propulsion

4.1 History background

The idea of using an electric propulsion based engine on spacecraft can be dated back to 1906 when Robert Goddard considered its possible use for space missions and when Konstantin Tsiolkovsky first formulated the Rocket equation law.

The development of first electric propulsion thrusters date back to 1960s: first experiments of electric thrusters occurred on 1964 with the SERT-1 (Space Electric Rocket Test 1) that proved the possibility of obtaining thrust through an electric thruster (therefore capable of delivering substantial current and applying it for space missions), and with the soviet satellite Zond-2 that mounted a Pulsed Plasma Thruster (PPT) aboard.

Despite these preliminary tests, first electric thrusters were developed only during 90s and were first applied to spacecraft in the following decade, when EP reached its full potential due to the advancing technology and increasing available power on board the spacecrafts.

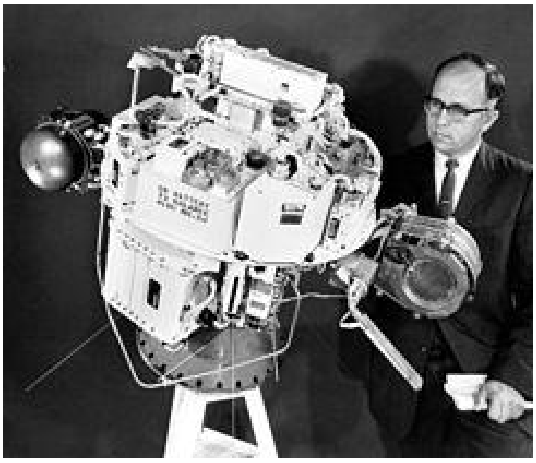

Figure 15: SERT-1

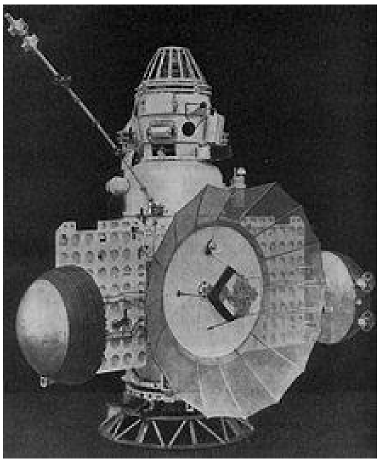

Figure 16:Zond-2

4.2 Fundamentals of Electric propulsion

Electric propulsion lies on the momentum conservation law: within some problem domain, the momentum remains constant and, therefore, it's neither created nor destroyed but, through the action of a force (thrust) the momentum can be changed (described by Newton's law of motion). Through the ejection of matter (e.g. high speed exhausted gas) in a specific direction, the spacecraft will respond by accelerating in the opposite direction (principle of action and reaction).

$$m\frac{dv}{dt} = \frac{dm}{dt}c$$

Table 2: Momentum conservation law terms

m	Time varying (instantaneous) mass of the vehicle
$\frac{dv}{dt}$	Spacecraft acceleration
c	Velocity of exhaust stream
$\frac{dm}{dt}$	Rate of change of spaceraft mass

$$T = \frac{dm}{dt}c$$

Table 3: Thrust terms

T	Thrust

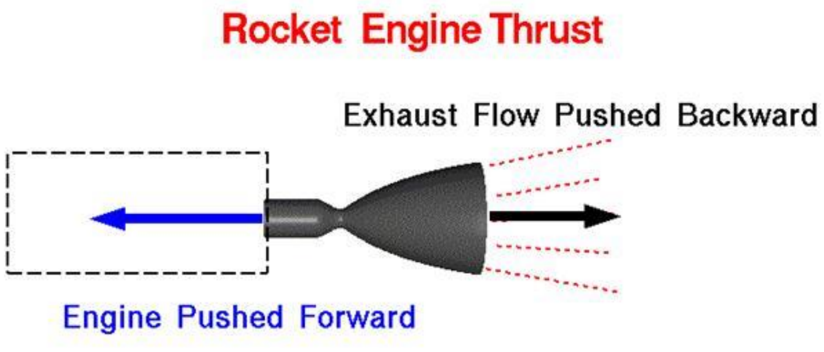

Figure 17: Rocket engine thrust

The thrust can be assumed as if it was an external force applied to the vehicle: the integral of thrust over time is the impulse (or change of momentum).

The key point for EP that distinguish it from CP, is that it achieves a value of propellant exhaust speed high because a large amount of energy can be transferred from the power source to the propellant.

A low amount of propellant is the main advantage of the EP because a high exhausted velocity directly translates in low amount of propellant consumption.

CP, instead, converts chemical energy from the propellant to kinetic energy and so, propellant consumption is higher.

Electric propulsion does not have energy limitations: by ignoring the components deterioration, the energy provided by solar panels and power source to a small amount of propellant is definitely bigger than the one provided with chemical propulsion.

The only limitation in energy quantity with electric propulsion lies in the solar panels and power source mass. However, the specific impulse (I_{sp}) for the EP is bigger and, therefore, electric propulsion based engines can provide thrust for longer time (up to few years) using less quantities of propellants.

EP has a big disadvantage that makes it less attractive when the mission length is short: the limitations on power source reduce the available thrust so thrust is defined as “low”. The consequence is that the operational times are long and that makes it difficult for short-timed missions.

A key term in the study of electric propulsion is the specific impulse: it is the ratio of thrust over the ration of expelled propellant measured in units of weight expelled per second.

$$I_{sp} = \frac{T}{W} = \frac{c}{g_0}$$

Table 4: Specific impulse law terms

I_{sp}	Specific impulse
$W = \frac{dm}{dt} g_0$	Rate of expulsion of propellant
g_0	Gravitational acceleration at sea level

Electric propulsion has specific impulse 10 times greater than the specific impulse obtained through the chemical propulsion. The specific impulse can be described as a measure of how efficient a rocket uses propellant; by definition, it is the total impulse delivered per unit of propellant consumed and is dimensionally equivalent to the generated thrust divided by the propellant mass or weight flow rate (thus meaning it has units of velocity).

A propulsion system with a high specific impulse uses the propellant mass way more efficiently in creating thrust and, in case of rockets, less propellant for a given ΔV. If the exhaust velocity (c) is assumed constant during thrust, the spacecraft experiments an increment in velocity which is linearly dependent on the exhaust velocity and logarithmically dependent on the propellant mass ejected, because of the Tsiolkovsky rocket equation:

$$\Delta V = c \ln \frac{m_0}{m_f}$$

Table 5: Tsiolkovsky rocket equation terms

ΔV	Increment in velocity
c	Velocity of exhaust stream
m_0	Initial total mass
m_f	Final total mass without the propellant

Electric spacecraft propulsion systems create thrust by using electric, and possibly magnetic, processes to accelerate a propellant. More intense forms of propellant heating, as used in electrothermal propulsion systems, offer one possibility for increased exhaust velocity, but encounter limitations due to restrictions on the temperatures that can be sustained by engine components in contact with the propellant gas flow. Thermodynamic expansion can be abandoned in favour of direct application of body forces to particles in the propellant stream. This is the method used by electrostatic and electromagnetic propulsion systems.

4.3 Thrusters classification

The principle of EP consists in applying electrical energy to the propellant from an external power source to obtain a high exhaust speed well above what the chemical propulsion engines produce. EP thrusters are classified in three main categories, according to the way they transfer energy to the propellant and the way that thrust and specific impulse are generated (that is to say how the plasma is accelerated).

- *Electrothermal propulsion:* the propellant in the chamber is heated thanks to an electrical component (e.g. a resistance) up to a specific temperature. The momentum on the spacecraft is imposed after the heat gas is accelerated through a nozzle where the thermal energy is transformed in kinetic energy.
- *Electrostatic propulsion:* the propellant is first ionized thanks to a power source, then it is accelerated by means of electrodes in the direction of the applied electric field.
- *Electromagnetic propulsion:* the propellant is ionized thanks to a power source, then it is accelerated thanks to the combined action of applied electric field and magnetic one (electric and magnetic forces).

Reistojets - Arcjets

In resistojets propellant in the chamber is heated by means of an electric resistance powered with electric energy. Heat passes from the resistance to the propellant through the mechanism of convection or irradiation. There are two main configurations:

- *Direct contact:* the resistance is in contact with the flow; heat passes from resistance to propellant through convection mechanism.
- *Sealed cavity:* resistance stays in a sealed cavity. Heat passes from resistance to propellant through irradiation mechanism, avoiding any sort of breaking mechanisms. For this configuration, it is necessary to over-heat the resistance because of the heater walls.

Resistojets have low specific impulses (I_{sp}) because the temperature of the gas is lower than the temperature of the resistance, high efficiency, limited power so they are used for not very demanding missions (orbit insertion and station keeping), thery are simple, cheap and reliable.

Arcjets have been developed to overcome the limitations on temperature of resistojets (where gas temperature is lower than resistance one). The propellant is first ionized or partially ionized, then the heat is deposited directly in the propellant (that becomes itself a conductor) where the current flow generates an electric arc. The arc heats the propellant in a not uniform way so that close to the propeller walls, the propellant has a lower temperature.

- A potential difference is applied to the ionized gas so that all the electrons reach the same value of current j.
- A ripple effect establishes a mechanism of collisions between electrons and atoms that results to the ionization of atoms first (because first ionization energy ϵ_{ij} of electrons is greater). It follows that the current grows rapidly with a non-linear trend.
- The electric field E accelerates the ions towards the cathode that emits electron because of the ions bombing.
- Sparkling potential V_C is reached (up to a thousand Volts): a sudden discharge is born and the current j tends to infinite, so it is necessary to limit it value by decreasing the potential with a luminescence discharge.
- The cathode needs to be heaten so it starts to emit ions by thermionic effect. The value of current j increase up to generate an electric arc.
- Temperature is about 10.000K (far from propeller walls), number of collisions increases and potential needs to decrease.

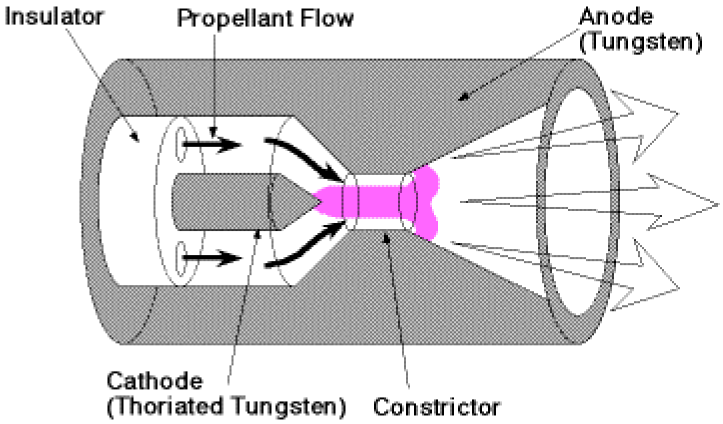

Figure 18: Arcjet

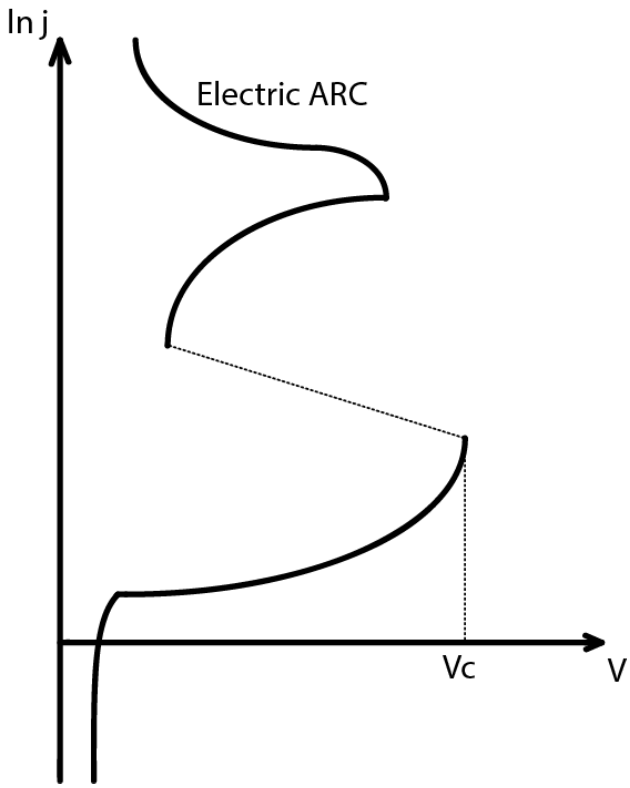

Figure 19: Arcjet,V vs ln j

Table 6: Resistojets performance

Propellant	N_2H_4	NH_3
I_{sp} $[s]$	300	350
P_E $[W]$	500-1500	500
η	0.8	0.8
Voltage	28	28
Thruster mass [kg/KW]	1-2	1-2
PPU mass [kg/KW]	1	1
Feed system	Blowdown	Regulated
Lifetime [h]	500	-
Missions	SK, orbit insertion, deorbit	Orbit corrections

Table 7: Arcjets performance

Propellant	N_2H_4	NH_3	H_2
I_{sp} $[s]$	500-600	500-800	1000
P_E $[W]$	300-2000	500-30k	5k-100k
η	0.35	0.3	0.4
Voltage	100	100	200
Thruster mass [kg/KW]	0.7	0.7	0.5
PPU mass [kg/KW]	2.5	2.5	2.5
Feed system	Regulated	Regulated	Regulated
Lifetime [h]	1000	1500	-
Missions	SK	SK, orbit raising	Medium ΔV transfers

Gridded Ion thrusters

The gridded ion thruster is a type of electrostatic thruster capable of generating low thrust levels with very high efficiency. This type of propeller exploits the acceleration of ions in the chamber thanks to the presence of high-voltage electrodes, capable of generating electrostatic forces that push the ions in the axial direction. The first applications date back to the nineties when engines of this type were mounted on board the Deep Space 1 probe.

The operating principle is as follows:

- The propellant (not yet ionized) atoms are sprayed into the chamber where an electronic cannon bombards them causing the electrons to be removed from the propellant atoms. The propellant is then ionized and positively charged, while the propeller walls absorb the lost electrons.
- The positively charged ions move to the chamber outlet because of diffusion, they escape into a plasma casing just above the positively charged grid.
- The ions are trapped between the two grids (positively and negatively charged respectively). They are accelerated in the direction of the negatively charged grid and then expelled in outer space.
- Electrons are fired through the ions by a cathode, called a neutralizer, to ensure that an equal amount of positive and negative charges is expelled. Neutralization is necessary to prevent the ship from gaining a net negative charge.

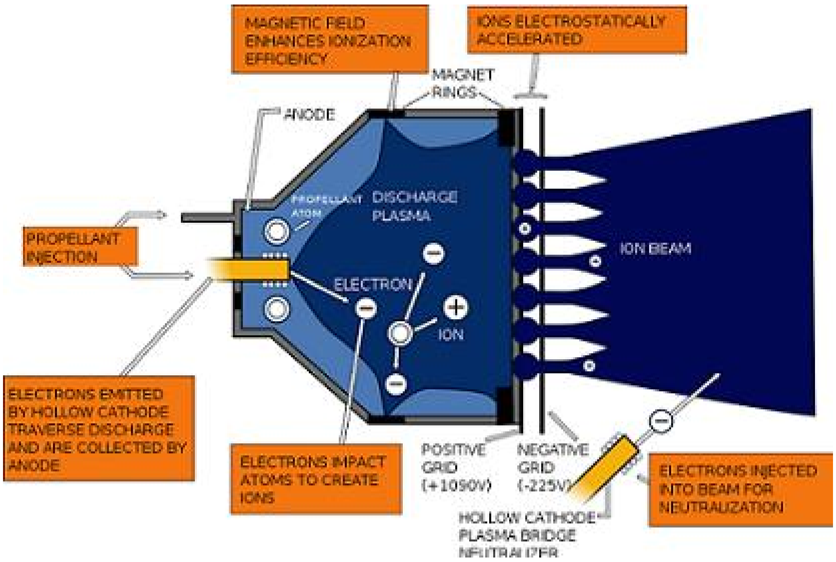

Figure 20: Diagram of a Gridded Ion Thruster

Hall thrusters

Hall thrusters or Stationary plasma thrusters is a hybrid between electrostatic and electromagnetic propulsion. This type of engine has the great advantage of not being subject to the limitation on the thrust density imposed by the Child law:

$$j_{max} = \frac{4\epsilon_0}{9}\sqrt{\frac{2q}{m_+}}\frac{V_G^{1.5}}{x_a^2}$$

which is the distinctive limit of the ion thrusters (because of a close-to-neutral plasma in the chamber and therefore there is no separation of charges).

The Hall effect thrusters base their operating principle on the acceleration of a working fluid (propellant) conveniently ionized by the mutual action of the superposition of a magnetic field and an electric field orthogonal to each other and directed respectively radially and along the axis of the propeller usually realized with cylindrical symmetry.

An electron discharge current is emitted from the cathode such that it flows in an almost axial direction towards the anode. When the electrons penetrate inside the thruster and are affected by the radial magnetic field they remain trapped in the zone of maximum intensity of the magnetic field which practically stops their motion towards the anode due to the small cyclotron radius of the electrons and gives them an azimuth speed creating a circumferential electronic current inside the propeller by Hall effect.

The magnetic force to which the electron is subject is given by:

$$F_B = qv_e \times B = qE = \frac{J_e}{n_e} \times B$$

The electron is subject to a result of the null forces because the electrostatic force equals the magnetic force:

$$-qE_z = qBv_\theta$$

There is only a Hall current j_θ equal to:

$$j_\theta = -n_e q v_\theta$$

The discharge is constituted by a high density of high energy electrons and allows ionization of the propellant, generally injected into the thruster through an annular distribution chamber constituted by the same anode, by means of the impact of the electrons with the working atoms. At each collision the electron advances generating a current towards the anode.

The distribution of electrons in the discharge produces a negative spatial discharge effect (virtual cathode) which generates a potential difference with the anode allowing the acceleration of the produced ions. For this reason, a current of ions is generated: the Hall effect thrusters are also defined as non-grid ion motors.

The ions accelerated by the potential difference are not affected by the action of the magnetic field (B) due to both their high atomic mass and their low speed, presenting a large radius of cyclotron and thus traveling along almost straight rectilinear paths mainly along the axis of the motor. The ions are then accelerated by the electromagnetic field in the axial direction.

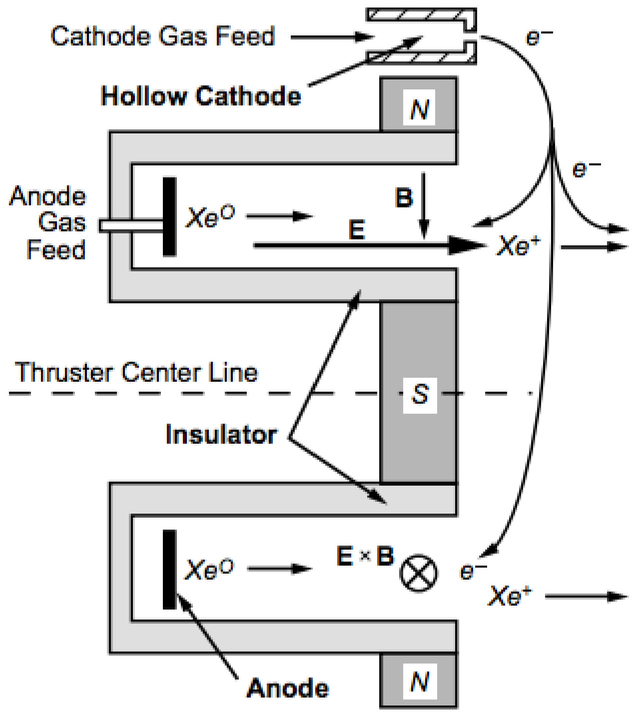

Figure 21: Hall thruster

Compared to ion propellers, Hall effect ones have a higher thrust density, a much lower ionization cost. They are suitable for missions characterized by specific pulses lower than those of missions for which ion thrusters are typically used.

However, plasma is an unstable environment: in fact, it can cause electromagnetic interference or radio-frequency interference and erosion of the internal surfaces of the engine; the performances can be influenced by the impact of the ions against the walls of the engine, the divergence of the beam, the presence of double ions.

Table 8: Hall thrusters vs Ion thrusters performance

Type	$Hall$	Ion
Propellant	Xe	Xe
I_{sp} $[s]$	1500-2500	2000-4000
P_E $[W]$	300-6000	200-5000
η	0.5	0.65
Voltage	200-600	1000-2000
Thruster mass [kg/KW]	2-3	3-6
PPU mass [kg/KW]	6-10	6-10
Feed system	Regulated	Regulated
Lifetime [h]	>7000	>10000
Missions	SK, orbit transfer (medium ΔV)	SK, orbit transfer (large ΔV)

MPD

A magnetoplasmadynamic (MPD) thruster (MPDT) is a form of electrically powered spacecraft propulsion which uses the Lorentz force (the force on a charged particle by an electromagnetic field) to generate thrust. It is sometimes referred to as Lorentz Force Accelerator (LFA) or (mostly in Japan) MPD arcjet (as an evolution of them). NASA refers to it as the "the most powerful form of electromagnetic propulsion"

Generally, a gaseous material is ionized and fed into an acceleration chamber, where the magnetic and electrical fields are created using a power source. The particles are then propelled by the Lorentz force resulting from the interaction between the current flowing through the plasma and the magnetic field (which is either externally applied, or induced by the current) out through the exhaust chamber. Unlike chemical propulsion, there is no combustion of fuel. As with other electric propulsion variations, both specific impulse and thrust increase with power input, while thrust per watt drops.

There are two main types of MPD thrusters, applied-field and self-field. Applied-field thrusters have magnetic rings surrounding the exhaust chamber to produce the magnetic field, while self-field thrusters have a cathode extending through the middle of the chamber. Applied fields are necessary at lower power levels, where self-field configurations are too weak. Various propellants such as xenon, neon, argon, hydrogen, hydrazine, and lithium have been used, with lithium generally being the best performer.

MPD thruster has two metal electrodes: a central rod-shaped cathode and a cylindrical anode surrounding the cathode. As for the arcjet, an electric arc is struck between anode and cathode thanks to high current. As the cathode heats up, it emits electrons that collide with ionized propellant to generate plasma. A magnetic field is created by the electric current returning to the power supply through the cathode, just like the magnetic field that is created when electrical current travels through a wire

According to Edgar Choueiri magnetoplasmadynamic thrusters have input power 100–500 kilowatts, exhaust velocity 15–60 kilometers per second, thrust 2.5–25 newtons and efficiency 40–60 percent.

One potential application of magnetoplasmadynamic thrusters is the main propulsion engine for heavy cargo and piloted space vehicles for long-term missions such as for Moon and Mars exploration, outer planet rendezvous.

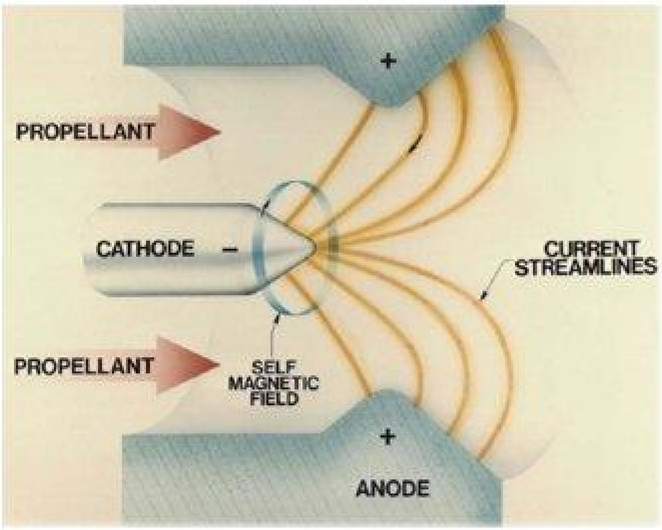

Figure 22: MPD thruster

Table 9: PPT vs AF-MPD vs SF-MPD performance

Type	PPT	AF-MPD	SF-MPD
I_{sp} $[s]$	500-1000	2000-5000	2000-5000
P_E $[W]$	1-200	1k-100k	200k-4M
η	0.1	0.5	0.3
Voltage	1000-2000	200	100
Thruster mass [kg/KW]	120	-	-
PPU mass [kg/KW]	100	-	-
Lifetime [h]	10^7 pulse	-	-
Missions	Precise corrections	Large ΔV (medium P_E)	Large ΔV (large P_E)

VASIMR

The VASIMR (Variable Specific Impulse Magnetoplasma Rocket) is a new type of electromagnetic thruster. Gases like xenon, argon or hydrogen are injected into a tube surrounded by superconducting magnets and a series of two radio wave couplers. The couplers have the function of ionizing the gas and, therefore, convert the cold gas into super heated plasma and the magnetic nozzle, in turn, converts the thermal motion of the plasma into a directional jet. The method by which the VASIMR generates thrust derives from research on nuclear fusion.

The first coupler is the helicon coupler that launches helical waves in the direction of cold gas and ionizes it. At this point the gas is a plasma but at a lower temperature than the operating temperature: for this reason it is called "cold plasma" (even if the temperatures reach 5800K). The second coupler is the ICH (Ion Cyclotron Heating) that allows to heat the plasma up to millions of K by means of waves thrown against the ions as they orbit around the magnetic field resulting in accelerated motion and an increase in temperature.

The motion of the ions takes place in a direction perpendicular to that of motion and it is necessary to modify its direction to generate thrust. This is possible thanks to the magnetic nozzle which converts the motion of the ions into useful linear momentum allowing the ions to reach speeds up to 180000 km / h.

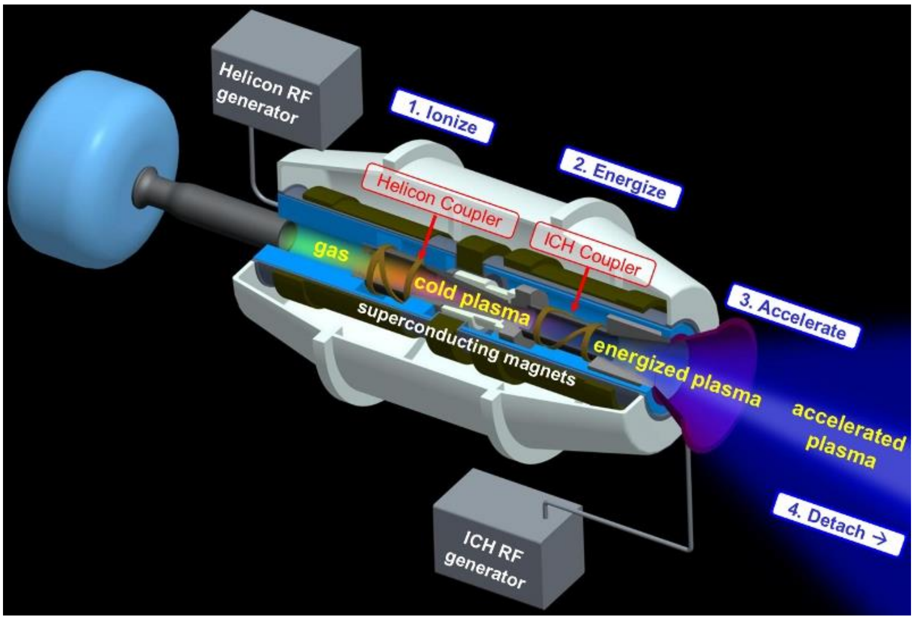

Figure 23: VASIMR

Pulsed Inductive Thrusters

Pulsed Inductive Thruster (PIT) was created to overcome the fundamental problem of electrode erosion in Pulsed Plasma Thrusters. The erosion is due to the high voltage of the formation of the discharge, to the high emission current of the electrodes, due to the bombardment of the ions flow and to the high temperature of the plasma. Specifically, electrode erosion is the factor that limits the useful lifetime of electromagnetic thrusters.

In this type of engine, this problem can be overcome by considering the coupling between the electrical energy impulse coming from the energy storage circuit, and the gas inductively, thus removing the direct physical contact between the electrodes and discharge into the plasma.

Therefore, the non-stationariety is used to obtain currents that vary over time, so as to exploit the phenomenon of mutual induction.

A PIT is basically constituted by a flat spiral induction coil, typically one meter in diameter, on which the gaseous propellant is injected.

Through this circuit a strong current impulse (100kA) is passed which rapidly leads to the growth of a magnetic field which permeates the gaseous propellant. According to Maxwell's law of induction, a corresponding electric field develops, whose module must be high enough to transform the gas into plasm, or in a state of high conductivity.

In turn, the magnetic field generates a secondary current inside the plasma opposite to the external current but in phase with it. The interaction between this secondary current and the magnetic field produces the magnetic force that allows the plasma to accelerate in the axial direction.

It is the current induced by the magnetic field that interacts profitably with the plasma. Each resistive current generated by the electric field is 90 degrees out of phase with respect to the magnetic field, so the corresponding magnetic force component reverses the sign every half cycle.

This engine is a promising system and the prototypes have provided encouraging results for applications such as primary propulsion in interplanetary missions. It has much higher returns than PPTs. The specific impulses are high:

$$I_{sp} = 4000 \div 9000\ s$$

As the accelerated plasma moves away from the external circuit, the effect of mutual induction decreases and therefore the accelerating force decreases in intensity. To solve this problem one could resort to a magnetic field traveling with the propellant. This device can be implemented by using alternately activated pairs of electrodes. A 1 megawatt system could pulse 200 times per second.

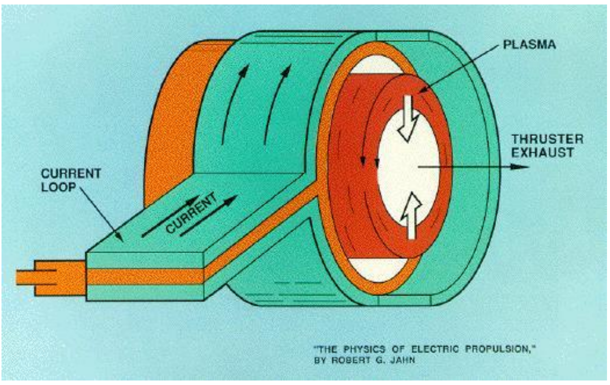

Figure 24: Pulsed Inductive Thruster (PIT)

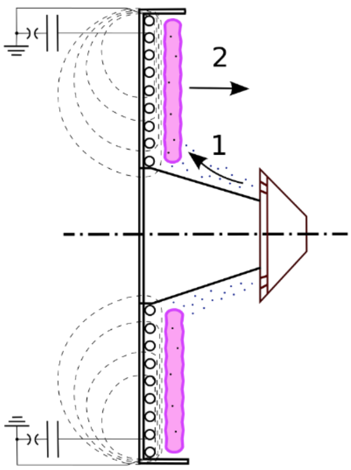

Figure 25: Propellant Injection Schematic

4.4 Propellants

Table 10: List of typical propellants for EP

	Pros	Cons
H_2	Low molecular mass $\mathscr{M}$	it dissociates easily, it is cryogenic and therefore difficult to preserve.
He	Low molecular mass $\mathscr{M}$	It is cryogenic and therefore difficult to preserve
Li	Low molecular mass $\mathscr{M}$	Toxic
NH_3	Liquid at room temperature, Low molecular mass $\mathscr{M}$ after dissociation. Easy to store.	It dissociates easily. Chemically reactive and requires vaporizer.
N_2H_4	Liquid at room temperature, Low molecular mass $\mathscr{M}$ after dissociation. Easy to store. exothermic dissociation	It dissociates easily and needs a gas generator.
H_2O	Easily storable. Great availability. Non-toxic and non-polluting.	It dissociates easily, needs a vaporizer and condensation must be avoided.

5 Results

The results for the space mission scenario about multiple debris removal with electric propulsion are here presented: the key point in the problem is the choice of electric propulsion onboard the chaser satellite instead of the chemical one.

Following the procedure summarized here, rendezvous times are first determined by studying the time at which the orbit planes of the debris coincide.

The procedure resulted in 109 combinations for acceleration values of $10^{-5}\ m/s^2$ and $10^{-6}\ m/s^2$ and 58 combinations for an acceleration equal to $10^{-7}\ m/s^2$ with time length shorter than 6 months, shown in Figure 9, Figure 10 and Figure 11.

The code has discarded regardless of those combinations that provided the chaser to return two or more times to the same debris. In addition, the code has rejected those combinations of debris that provided a time of rendezvous between one debris and another lower than the thrust time.

This is because it would be impossible to reach a debris with electric propulsion with thrust time greater than transfer time.

Results for the J2 perturbations on the orbital element Ω for the debris sequence "27819 – 25893 – 8326 – 11309" show how the RAAN is perturbed daily of:

NORAD No.	Daily perturbation of Ω [°/day]
27819	-0.0984
25893	-0.0887
8326	-0.0072
11309	-0.1150

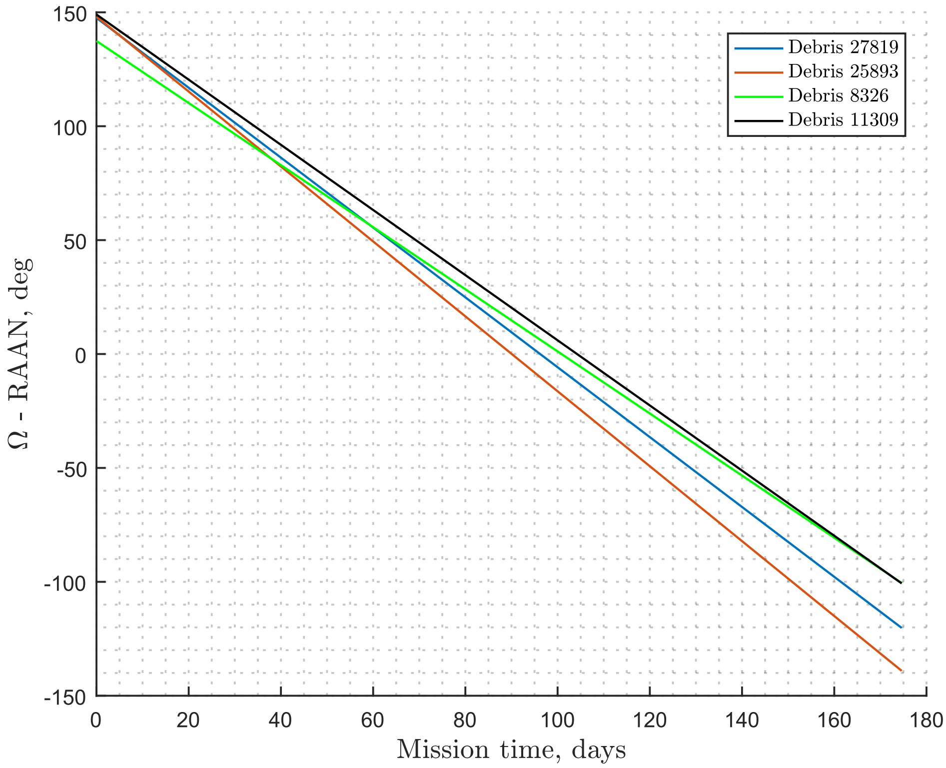

*Figure 26:**Ω** perturbation for the debris combination over the mission time*

This will directly influence the time for rendezvous and proximity operations. By imposing $t = 0\ days$ the departure time from the debris and $\Delta\Omega = \Omega_i - \Omega_j = 0$ (between the departure debris and the arrival one), the condition for performing a correct rendezvous, the thrust time is finite and should be properly chosen to catch the debris at the right time and place.

For each of the 109 (or 58) combinations, time-related data, consumption data (in terms of ΔV of individual legs and complete transfer) and data related to the de-skid planes offset were printed on output files.

Among all the provided solutions, the same sequences were analysed for electric propulsion and for chemical propulsion, evaluating the differences in terms of mission time and consumption, propellant consumption and solar arrays mass (for the three types of EP thrusters only).

5.1 *Output tables with dimensional results*

In the following pages, there will be presented the results according to the analysis of a space mission about multiple debris removal with an electric propulsion based chaser.

Input data for the analysis started by imposing multiple acceleration values to satisfy the different thrust on mass ratios for different propulsion engines.

Table 11: Thrust on mass ratios (Acceleration)

Acceleration [m/s^2]
$1 \cdot 10^{-6}$
$1 \cdot 10^{-7}$
$1 \cdot 10^{-5}$

The mass of the spacecraft is the sum of the mass of the chaser, that of the kit and the mass of the solar panels.

Starting from the necessary output power, technology level and efficiency the mass for the solar panels has been calculated as follow:

$$P = \frac{T \cdot I_{sp} \cdot g_0}{2\eta}$$

$$m_{solar\ panels} = \frac{\left(\beta \cdot T \cdot I_{sp} \cdot g_0\right)}{2\eta} = \beta \cdot P$$

where

- $\beta = 30\ kg/kW$
- $I_{sp} = 3000\ s\ (Ion), 1800\ s\ (Hall), 600\ s\ (Arcjet)$
- $g_0 = 9.8\ m/s^2$
- $a = 1 \cdot 10^{-6}\ m/s^2, 1 \cdot 10^{-7}\ m/s^2, 1 \cdot 10^{-5}\ m/s^2$

- $\eta = 0.65\ (Ion), 0.5\ (Hall), 0.35\ (Arcjet)$

$$m_{SC} = m_{chaser} + m_{kit} + m_{solar\ panels} \cong 2500\ kg$$

This result for the mass of the spacecraft is an approximation due to the unknown value of the solar panel mass and it's been the starting point for the mass budget calculation (specific results are presented in the following pages).

The mass of the solar panels considers only the chaser, because, as already mentioned, the kit is equipped with chemical propulsion.

The deorbit phase is supposed with chemical propulsion: deorbit with electric propulsion is more economical in terms of ΔV, but would provide considerable mission time and human resources in terms of mission control operators as well as the exact calculation of the point of re-entry into the atmosphere remains an unknown factor of the problem.

Table 12: Solar panel mass and Power for $a = 1 \cdot 10^{-5}\ m/s^2$

Engine type	**Solar panel mass $[kg]$**	**Power $[W]$**
Ion	17	565
Hall	13.23	441
Arcjet	6.3	210

Table 13: Solar panel mass and Power for $a = 1 \cdot 10^{-6}\ m/s^2$

Engine type	**Solar panel mass $[kg]$**	**Power $[W]$**
Ion	1.7	56.5
Hall	1.32	44
Arcjet	0.63	21

Table 14: Solar panel mass and Power for $a = 1 \cdot 10^{-7}\ m/s^2$

Engine type	**Solar panel mass $[kg]$**	**Power $[W]$**
Ion	0.17	5.6
Hall	0.13	4.5
Arcjet	0.06	2

The power generated by the ion thrusters, in the 3 different scenarios, is bigger, as the specific impulse (I_{sp}) is greater than the Hall thrusters and Arcjets, and so the mass of the solar panels for ion thruster is bigger, taking into account the same technological level (β) for all the three thrusters.

Each of the output files was organized on a calculation page on Excel and all the combinations of four debris were compared.

For all the three acceleration estimation, the results in terms of minimum consumption and maximum consumption are the same; the inequality was found in the thrust time for the multiple transfers.

This is obviously a direct consequence of the divergence in the acceleration quantities.

- For the acceleration value of $1 \cdot 10^{-6}\ m/s^2$ thrust time requires few days (2 to 5 days) for burning.
- For the acceleration value of $1 \cdot 10^{-7}\ m/s^2$ thrust time requires tens of days (12 to 44 days) for burning.
- For the acceleration value of $1 \cdot 10^{-5}\ m/s^2$ the thrust time is significantly lower, that is to say few hours (less than an hour to 10 hours) for burning.

Table 15: Mean thrust time for different acceleration values

Acceleration $[m/s^2]$	**Mean thrust time [days]**
10^{-6}	3.012
10^{-5}	0.301
10^{-7}	28.502

The electric propulsion transfers with the lowest acceleration value of $10^{-7} m/s^2$ appear to be problematic as the mean evaluated thrust time is greater, compared to the other two studied cases ($a = 1 \cdot 10^{-6}\ m/s^2$ and $a = 1 \cdot 10^{-7}\ m/s^2$).

This parameter needs to be compared with the time necessary for the orbit planes to coincide, that is to say the time necessary for the rendezvous.

For this reason, the four-debris combinations with that specific acceleration quantity ($a = 1 \cdot 10^{-7}\ m/s^2$) are less in number than the other two cases.

The total consumption (in terms of ΔV) for the entire mission is the same for the three studied cases considering that the ΔV does not depend on the acceleration of the spacecraft but only on the perturbed variation of semi-major axis and orbit eccentricity.

Table 16: Best Three-Leg Missions in Terms of ΔV for $a = 1e - 06\ m/s^2$

Sequence	NORAD No.				Trip time, days	ΔV, km/s
	#1	**#2**	**#3**	**#4**		
1	27819	25893	8326	11309	194.620	0.21866
2	27466	27535	11170	10777	183.735	0.45444
3	13066	11170	27535	28421	151.769	0.45709
4	27535	27466	13003	28910	192.889	0.48999
5	27466	27535	11170	28421	191.091	0.50248

Table 17: Best Three-Leg Missions in Terms of ΔV for $a = 1e - 05\ m/s^2$

Sequence	NORAD No.				Trip time, days	ΔV, km/s
	#1	**#2**	**#3**	**#4**		
1	27819	25893	8326	11309	194.620	0.21866
2	27466	27535	11170	10777	183.735	0.45444
3	13066	11170	27535	28421	151.769	0.45709
4	27535	27466	13003	28910	192.889	0.48999
5	27466	27535	11170	28421	191.091	0.50248

Table 18: Best Three-Leg Missions in Terms of $\boldsymbol{\Delta V}$ for $\boldsymbol{a = 1e-07\ m/s^2}$

Sequence	**NORAD No.**				**Trip time, days**	**ΔV, km/s**
	#1	**#2**	**#3**	**#4**		
1	27819	25893	8326	11309	205.2096	0.21866
2	27466	27535	11170	10777	183.735	0.45444
3	13066	11170	27535	28421	173.1984	0.45709
4	27466	27535	11170	28421	191.0910	0.50248
5	16511	27870	11170	10777	163.735	0.50714

Table 19: Best Three-Leg Missions in Terms of Trip Time $\boldsymbol{\Delta t}$ for $\boldsymbol{a = 1e-06\ m/s^2}$

Sequence	**NORAD No.**				**Trip time, days**	**ΔV, km/s**
	#1	**#2**	**#3**	**#4**		
1	13066	13003	27535	11170	123.8727	0.84296
2	27535	27466	13003	21090	125.15942	0.73455
3	13066	13003	27535	27870	126.37418	0.99733
4	13003	13066	27870	27535	126.37418	0.88459
5	11170	13066	27870	27535	126.37418	0.61615

Table 20: Best Three-Leg Missions in Terms of Trip Time $\boldsymbol{\Delta t}$ for $\boldsymbol{a = 1e - 05\ m/s^2}$

Sequence	**NORAD No.**				**Trip time, days**	**ΔV, km/s**
	#1	**#2**	**#3**	**#4**		
1	13066	13003	27535	11170	123.8727	0.84296
2	27535	27466	13003	21090	125.15942	0.73455
3	13066	13003	27535	27870	126.37418	0.99733
4	13003	13066	27870	27535	126.37418	0.88459
5	11170	13066	27870	27535	126.37418	0.61615

Table 21: Best Three-Leg Missions in Terms of Trip Time $\boldsymbol{\Delta t}$ for $\boldsymbol{a = 1e - 07\ m/s^2}$

Sequence	**NORAD No.**				**Trip time, days**	**ΔV, km/s**
	#1	**#2**	**#3**	**#4**		
1	11170	13066	27870	27535	151.31328	0.61615
2	11170	13066	28421	27535	153.58982	0.61779
3	11170	13066	27870	10777	162.34808	0.62282
4	27870	16511	28421	27535	168.48352	0.76246
5	27535	27466	10777	27870	169.16294	0.77037

Interesting results can be found in the “best three-leg missions in terms of mission time” tables for the different acceleration values: in fact, the first four best sequences for the acceleration equal to $1 \cdot 10^{-6}\ m/s^2$ and $1 \cdot 10^{-5}\ m/s^2$ (13066, 13003, 27535, 11170 – 27535, 27466, 13003, 21090 – 13066, 13003, 27535, 27870 – 13003, 13066, 27870, 27535) does not appear in the best five sequences for the acceleration value of $1 \cdot 10^{-7}\ m/s^2$ where the best sequence in terms of trip time (11170,13066,27870,27535) is equal to the fifth best combination of four debris in the other two context.

Table 22: Minimum delta V for Electric Propulsion based engines

Acceleration $[m/s^2]$	**Minimum ΔV budget [km/s]**
10^{-6}	0.21866
10^{-5}	0.21866
10^{-7}	0.21866

Table 23: Maximum delta V for Electric Propulsion based engines

Acceleration $[m/s^2]$	**Maximum ΔV budget [km/s]**
10^{-6}	1.01078
10^{-5}	1.01078
10^{-7}	1.01078

The four-debris combinations that provide the minimum or maximum consumption for the space mission are, obviously, the same:

Table 24: Four-debris combination providing minimum delta V

27819	25893	8326	11309

Table 25: Four-debris combination providing maximum delta V

13066	13003	12092	27466

- 27819 is a SL-8 Rocket body, launched on June 4, 2003 from Plesetsk Missile and Space Complex (PKMTR)

- 25893 is a SL-8 Rocket body, launched on August 26, 1999 from Plesetsk Missile and Space Complex (PKMTR)

- 8326 is a SL-8 Rocket body, launched on September 24, 1975 from Plesetsk Missile and Space Complex (PKMTR)

- 11309 is a SL-8 Rocket body, launched on March 21, 1979 from Plesetsk Missile and Space Complex (PKMTR)

- 13066 is a SL-8 Rocket body, launched on February 17, 1982 from Plesetsk Missile and Space Complex (PKMTR)

- 13003 is a SL-8 Rocket body, launched on December 17, 1981 from Plesetsk Missile and Space Complex (PKMTR)

- 12092 is a SL-8 Rocket body, launched on December 10, 1980 from Plesetsk Missile and Space Complex (PKMTR)

- 27466 is a SL-8 Rocket body, launched on July 8, 2002 from Plesetsk Missile and Space Complex (PKMTR)

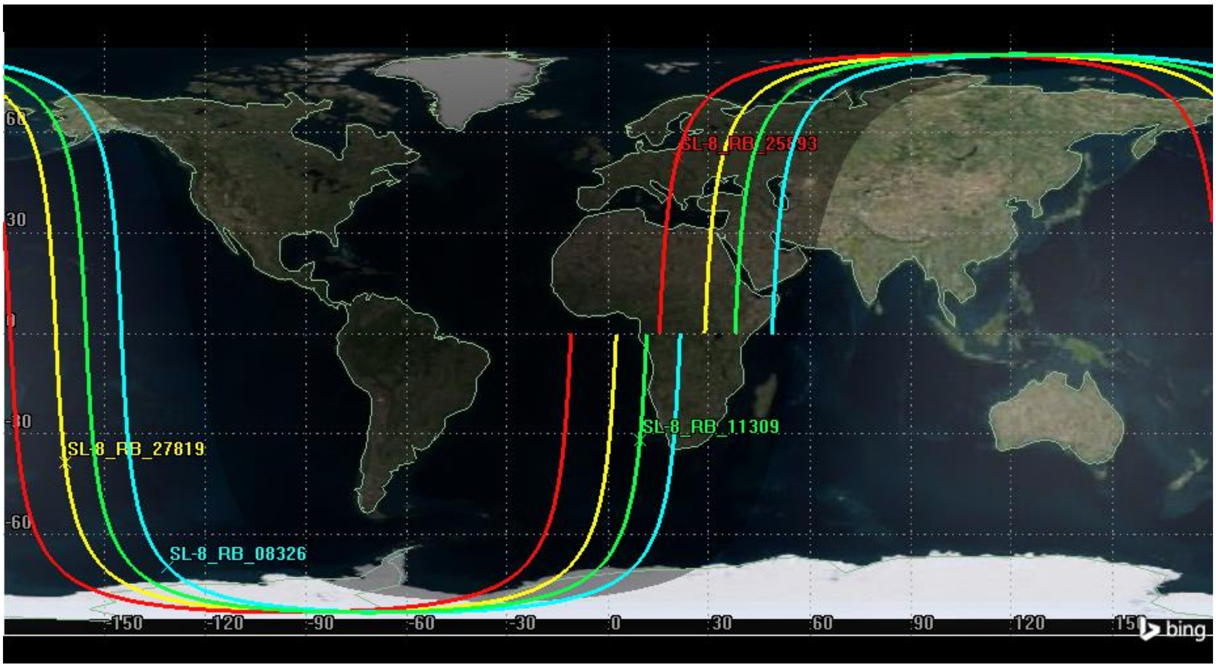

Figure 27: 2D Graphic (Ground track) of the four-debris

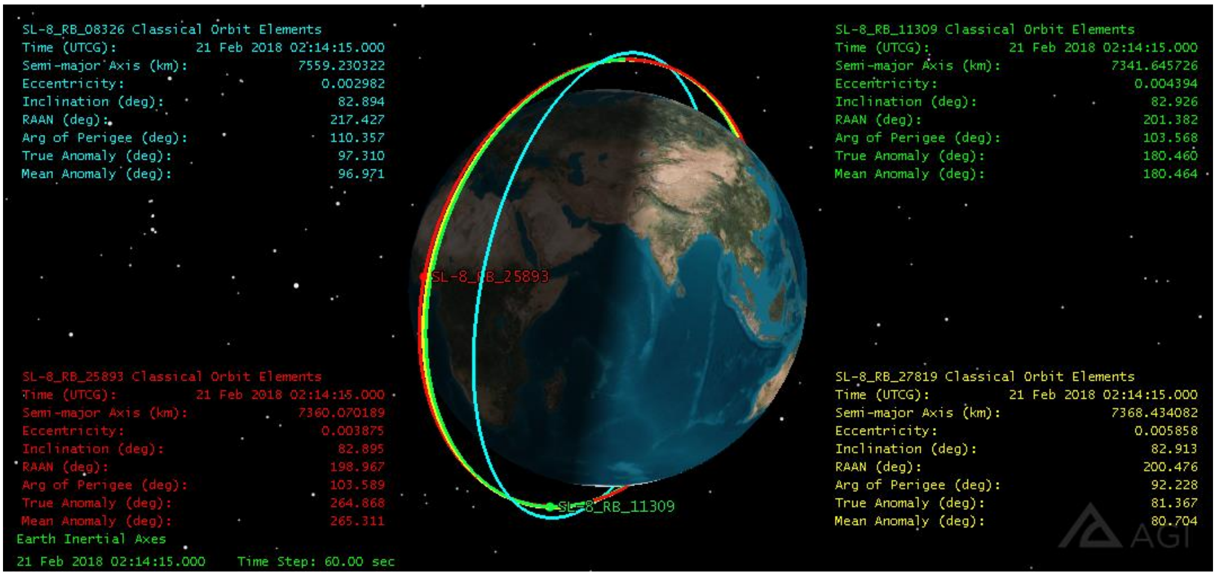

Figure 28: 3D Graphic (Orbit View) of the four-debris

The four-debris combinations that provide the minimum mission time are, contrarily, different for the three quantities of acceleration.

Table 26: Four-debris combination providing minimum mission time

Acceleration $[m/s^2]$				
10^{-6}	13066	13003	27535	11170
10^{-5}	13066	13003	27235	11170
10^{-7}	11170	13066	27870	27535

The minimum mission time with electric propulsion is the same for the acceleration values of 10^{-6} m/s^2 and 10^{-7} m/s^2, considering that the 4-debris combination is the same, while the minimum mission time for the lower acceleration value of 10^{-7} m/s^2 appears to be greater because of the different debris combination.

Table 27: Minimum mission time for Electric propulsion based engines

Acceleration $[m/s^2]$	**Minimum mission time [days]**
10^{-6}	123.8727
10^{-5}	123.8727
10^{-7}	151.31328

5.2 *Mass budget*

The table below shows the breakdown of the mass budget, providing the values for mission initial mass m_{start}, kit mass m_k and propellant consumed during each leg m_p for the sequences with trip time below 6 months (in terms of minimum and maximum). Values for power (P) have been considered only for electric propulsion cases.

The calculation of the masses for the space mission follows the assumption that the kit equipped with chemical propulsion based thruster employs a liquid propulsion system with specific impulse $I_{sp} = 310\ s$.

Mass budget breakdown has been calculated varying the specific impulses for the three type of electric thrusters for the three values of acceleration ($10^{-5}\ m/s^2, 10^{-6}\ m/s^2, 10^{-7}\ m/s^2$).

This is to say that only the chaser spacecraft mounts an electric propulsed thruster onboard while all the kits are equipped to perform thrust with chemical propulsion. An ion thruster ($I_{sp} = 3000s$), a Hall thruster ($I_{sp} = 1800s$) and arcjet ($I_{sp} = 600s$) are here considered.

Table 28: Mass budget breakdown for $\boldsymbol{a = 1 \cdot 10^{-5}\ m/s^2}$

	$\boldsymbol{Chaser\ I_{sp}\ [s]}$	$\boldsymbol{m_{start}\ [kg]}$		$\boldsymbol{m_k\ [kg]}$		$\boldsymbol{m_p\ [kg]}$	
		min	**max**	**min**	**max**	**min**	**max**
CP	310	2166	3817	164	275	9	423
Ion thruster	3000	2715	2971	164	275	1	35
Hall thruster	1800	2727	3015	164	275	2	60
Arcjet	600	2784	3314	164	275	6	194

Table 29: Mass budget breakdown for $\boldsymbol{a = 1 \cdot 10^{-6}\ m/s^2}$

	$\boldsymbol{Chaser\ I_{sp}\ [s]}$	$\boldsymbol{m_{start}\ [kg]}$		$\boldsymbol{m_k\ [kg]}$		$\boldsymbol{m_p\ [kg]}$	
		min	**max**	**min**	**max**	**min**	**max**
CP	310	2166	3817	164	275	9	423
Ion thruster	3000	2715	2971	164	275	1	35
Hall thruster	1800	2727	3015	164	275	2	60
Arcjet	600	2784	3314	164	275	6	194

Table 30: Mass budget breakdown for $\boldsymbol{a = 1 \cdot 10^{-7}\ m/s^2}$

	$\boldsymbol{Chaser\ I_{sp}\ [s]}$	$\boldsymbol{m_{start}\ [kg]}$		$\boldsymbol{m_k\ [kg]}$		$\boldsymbol{m_p\ [kg]}$	
		min	**max**	**min**	**max**	**min**	**max**
CP	310	2166	3817	164	275	9	423
Ion thruster	3000	2715	3314	164	275	1	194
Hall thruster	1800	2727	3314	164	275	2	194
Arcjet	600	2784	3314	164	275	6	194

5.3 Electric propulsion – Chemical propulsion comparison

There are two main differences between the electric propulsion and the chemical propulsion: the first one is the type of burn the spacecraft performs to make a manoeuvre because the thrust with the chemical propulsion needs an impulsive burn as the propellant requires it, while the thrust with the electric propulsion is performed with a finite burn considering that the spacecraft mounts a power source (a generator); the second difference lies in the estimation of the optimal transfer ΔV that can be expressed as:

$$\frac{\Delta V}{V} = 0.5\sqrt{\left(\frac{\Delta a}{a}\right)^2 + \Delta e^2}$$

where the change in semimajor axis Δa is considered and empirical relation and Δe is the additional eccentricity vector change.

Table 31: Comparison between EP and CP in terms of $\boldsymbol{\Delta V}$

	Minimum ΔV	Maximum ΔV
Chemical propulsion	0.21539	1.0076
Electric propulsion	0.21866	1.01078

Table 32: Comparison between EP and CP in terms of $\boldsymbol{t}$

	Minimum t	Maximum t
Chemical propulsion	103.8727	182.62815
Electric propulsion	103.8727	182.62815

Electric propulsion requires a slightly higher value for ΔV $[km/s]$ compared to that of the chemical propulsion: specifically, 1.5% more ΔV is required.

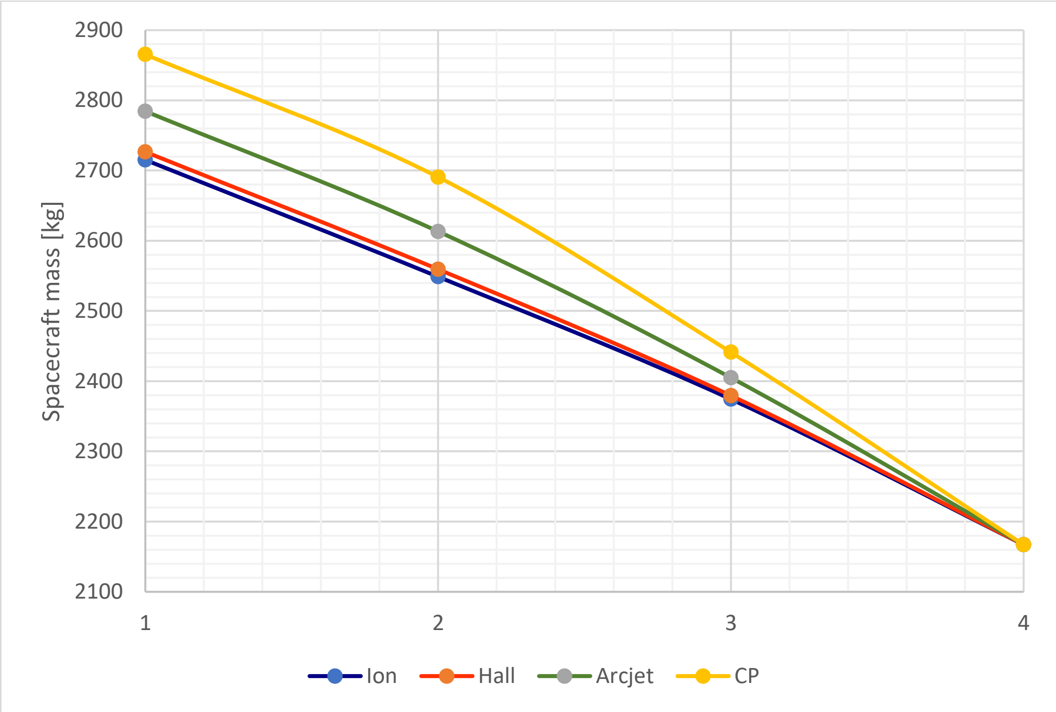

Figure 29: Spacecraft mass decrease during the best three-leg mission for CP and EP thruster, for all the acceleration values

In all three cases of acceleration, for the different types of engine, the mass of the spacecraft decreases with each leg because part of it is used in the kit that is released on the debris and part is in the propellant consumed to perform the rendezvous manoeuvres.

The ion thruster solution provides a lower initial mass for the spacecraft (2715.15 kg) compared to the other three cases of Hall thruster (2726.57 kg), arcjet (2784.52 kg) and chemical propulsion thruster (2865.37 kg).

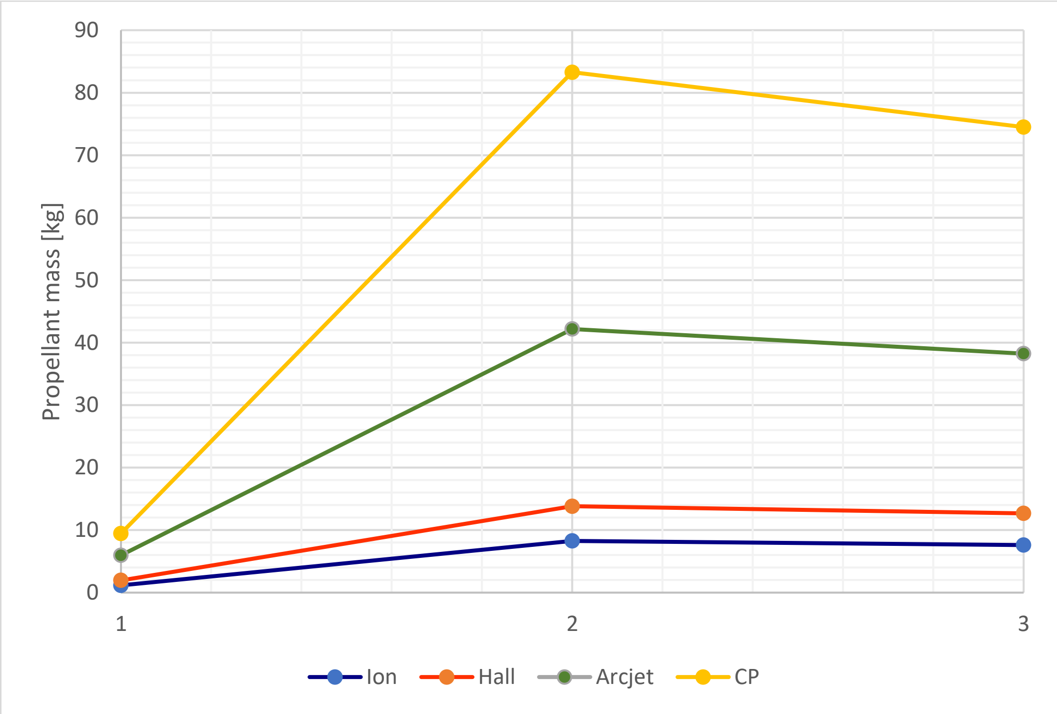

Figure 30: Propellant mass consumption for the best three-leg mission for CP and EP thruster, for all the acceleration values

From the graphs shown above, regarding the propellant consumption (in terms of kilograms of propellant necessary for the rendezvous manoeuvre), it is soon clear how the results for EP are considerably better than CP ones.

The high specific impulse (I_{sp}) of the electric thrusters in general allows up to 10 times saving of propellant.

Taking a look to the second of the three rendezvous manoeuvres, the propellant consumption evaluated for the chemical propulsion is 81.5 kg while, taking into account the best scenario with ion thrusters (greater I_{sp}), the propellant consumption is just 8.27 kg for all the three different acceleration values.

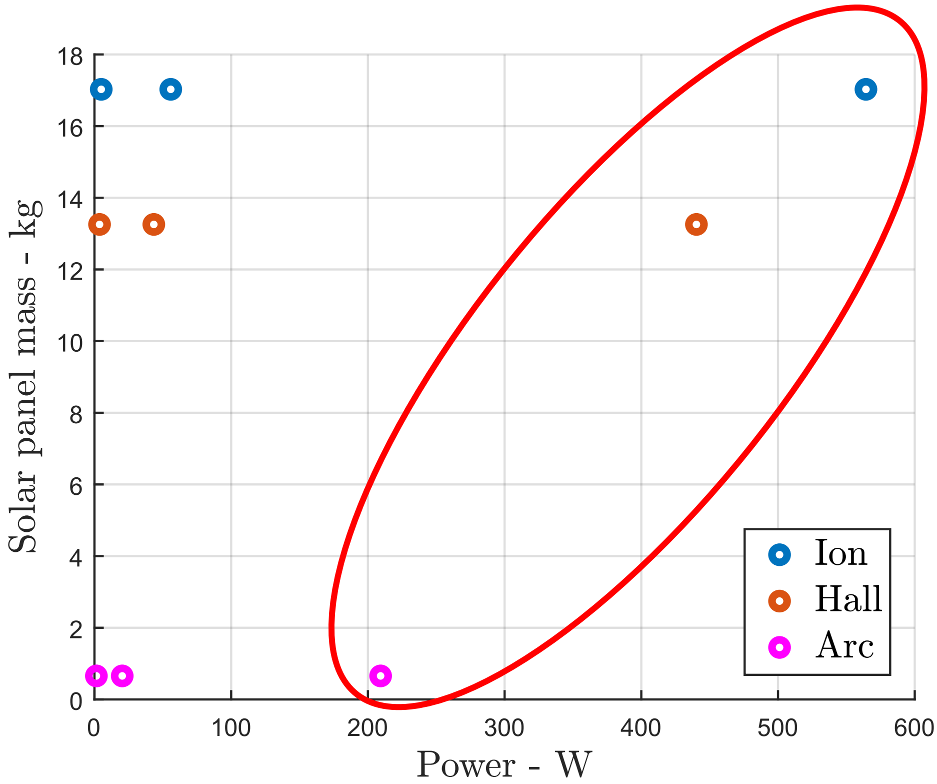

Figure 31: Power depending on Solar panel mass for the three electric thrusters

The Figure 31 represents an evaluation of the direct correlation between the necessary onboard power (P) and the required solar panel mass (m_p).

An almost linear trend is immediately visible: as the required onboard power increases, there is an increase in the mass of the solar panel.

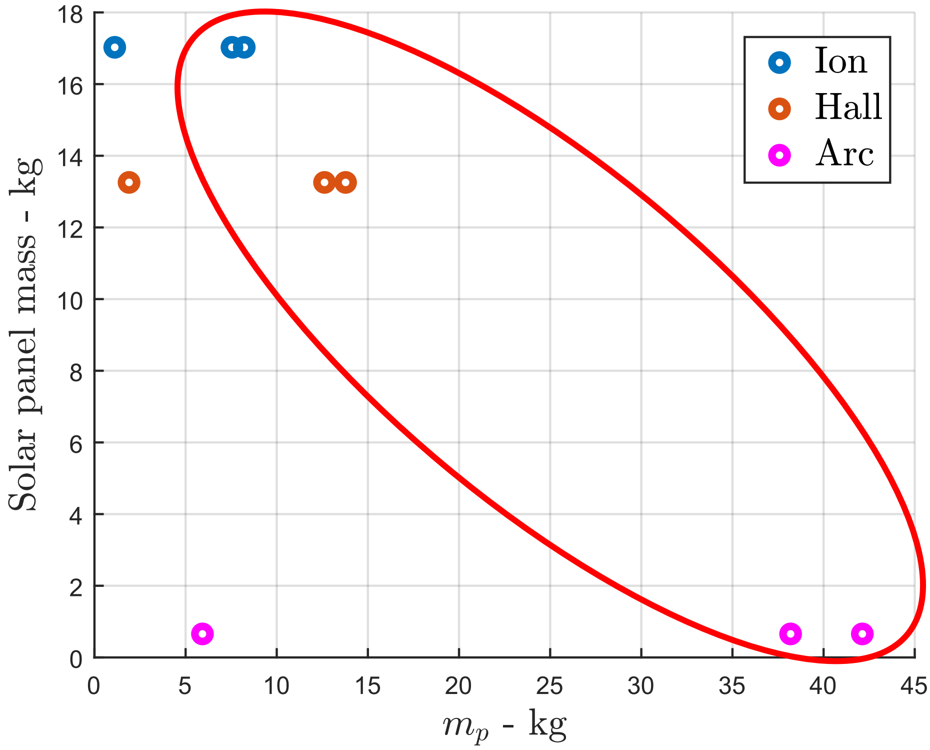

Figure 32: Propellant mass depending on Solar panel mass for the three electric thrusters

Figure 32, shows the trend of the mass of solar panel as a function of the propellant mass: a linear decreasing trend is immediately clear. As the mass of propellant increases, there is a decrease in the mass of the solar panels so that the mass of the spacecraft (which takes into account both masses) remains more or less constant.

Furthermore, an interesting comparison stays in the effective weight saving for the spacecraft equipped with electric propulsion, taking into account the gain in mass because of the propellant and the loss in weight due to the presence of solar panels.

The mass saving, for the EP thrusters, has been calculated as follow:

$$mass\ saving = \frac{m_{p_{CP}} - (m_p + m_{sp})}{m_{p_{CP}}} \cdot 100$$

Table 33: Propellant mass and solar panel mass for EP, $a = 1 \cdot 10^{-5}\ m/s^2$

	Leg 1	Leg 2	Leg 3	m_p saving [kg]	Solar panel mass [kg]	Mass saving [%]
	$m_p\ [kg]$					
CP	9.4623	83.28152	74.50974		--	
Ion thruster	1.16454	8.27016	7.59486	150.224	17	79.6
Hall thruster	1.9493	13.82912	12.67288	138.802	13.23	75
Arcjet	5.97564	42.17735	38.2414	80.859	6.3	44.5

Table 34: Propellant mass and solar panel mass for EP, $a = 1 \cdot 10^{-6}\ m/s^2$

	Leg 1	Leg 2	Leg 3	m_p saving [kg]	Solar panel mass [kg]	Mass saving [%]
	$m_p\ [kg]$					
CP	9.4623	83.28152	74.50974		--	
Ion thruster	1.16454	8.27016	7.59486	150.224	1.7	88.8
Hall thruster	1.9493	13.82912	12.67288	138.802	1.32	82.2
Arcjet	5.97564	42.17735	38.2414	80.859	0.63	48

Table 35: Propellant mass and solar panel mass for EP, $a = 1 \cdot 10^{-7}\ m/s^2$

	Leg 1	Leg 2	Leg 3	m_p saving [kg]	Solar panel mass [kg]	Mass saving [%]
	$m_p\ [kg]$					
CP	9.4623	83.28152	74.50974		--	
Ion thruster	1.16454	8.27016	7.59486	150.224	0.17	89.7
Hall thruster	1.9493	13.82912	12.67288	138.802	0.13	83
Arcjet	5.97564	42.17735	38.2414	80.859	0.063	48.3

With the use of electric propulsion onboard our spacecraft, we obtain benefits in terms of mass: in the face of mass spending on the installation of solar panels, we see a fuel saving that is so effective as to completely compensate the additional mass for solar panels.

With the use of ion thruster, the propellant gain reaches up to 90% while for the Hall thruster (the "worst case" for the EP) the gain reaches “just” the 48%.

The possibility of carrying out the mission with electric propulsion – with the same mission time – gives advantages both about the initial mass of the spacecraft and the mass of propellant to be carried on board.

6 References

Edelbaum, Theodore N. "Propulsion requirements for controllable satellites." *ARS Journal* 31.8 (1961): 1079-1089.

Bate, Roger R., Donald D. Mueller, and Jerry E. White. *Fundamentals of astrodynamics*. Courier Corporation, 1971.

CASALINO, Lorenzo; PASTRONE, Dario Giuseppe. *Mission Design and Disposal Methods Comparison for the Removal of Multiple Debris*. 2016.

RYCROFT, Michael J. Stengel; ROBERT, F. *Spacecraft Dynamics and Control*. 1997.

https://celestrak.com

http://sci.esa.int/smart-1/34201-electric-spacecraft-propulsion/?fbodylongid=1535

https://www.nasa.gov/centers/glenn/about/fs22grc.html

http://www.adastrarocket.com/aarc/VASIMR

http://www2.ee.ic.ac.uk/derek.low08/yr2proj/ion.htm

http://www.aerospacengineering.net/?p=537

https://www.nasa.gov/mission_pages/station/news/orbital_debris.html

7 Acknowledgments

I'd like to thank professor *Lorenzo Casalino* first, who guided me during this work, was always present and available for any clarification and in successfully indicating the way for the accomplishment of this thesis.

My thanks also go to the people who – in these years – have supported me, above all from afar, people who have been the lighthouse during the most difficult moments of my studies: my love *Simona* who loved and supported me in these years, who has always believed in me and has continuously encouraged me to reach this goal as soon as possible.

To my parents *Mariantonietta* and *Pierluigi* and my sister *Ilaria*, who contributed to my well-being, my tranquillity and my happiness here in Turin.

To my grandmother *Maria* who has faced for the second time a long trip, to personally attend my master thesis session, and to all my uncles and cousins who have decided, for a day, to abandon their daily duties and be present for this very important moment.

To all my friends, to the Cubesat team and all the professors and collaborators I have met during these here, thanks for giving me something useful for the success of this journey.

Farewell Politecnico, see you soon.